



50 years of balloon-borne ozone profile measurements at Uccle, Belgium: short history, scientific relevance and achievements in understanding the vertical ozone distribution

Roeland Van Malderen¹, Dirk De Muer¹, Hugo De Backer¹, Deniz Poyraz¹, Willem W. Verstraeten¹,
5 Veerle De Bock¹, Andy Delcloo¹, Alexander Mangold¹, Quentin Laffineur¹, Marc Allaart², Frans
Fierens³, Valérie Thouret⁴

¹Royal Meteorological Institute of Belgium, Uccle (Brussels), 1180, Belgium

²KNMI, P.O. Box 201, 3730 AE De Bilt, the Netherlands

³Belgian Interregional Environment Agency (IRCEL - CELINE), Brussels, 1030, Belgium

10 ⁴Laboratoire d'Aérologie, Université de Toulouse, CNRS, UPS, Toulouse, France

Correspondence to: R. Van Malderen (roeland.vanmalderen@meteo.be)

Abstract. Starting in 1969, and with three launches a week, the Uccle (Brussels, Belgium) ozonesonde dataset is one of longest and densest of the world. Moreover, as the only major change was the switch from Brewer-Mast to Electrochemical Concentration Cell (ECC) ozonesonde types in 1997 (when the emissions of ozone depleting substances peaked), the Uccle
15 time series is very homogenous. In this paper, we briefly describe which efforts have been taken during the first three decades of the 50 years of ozonesonde observations to guarantee the homogeneity between ascent and descent profiles, under changing environmental conditions (e.g. SO₂), and between the different ozonesonde types. This paper focusses on the 50 years long Uccle ozonesonde dataset and aims to demonstrate its past, present and future relevance to ozone research in two application areas: (i) the assessment of the temporal evolution of ozone from the surface to the (middle) stratosphere, and (ii)
20 as backbone for validation and stability analysis of both stratospheric as well as tropospheric satellite ozone retrievals. Using the Long-term Ozone Trends and Uncertainties in the Stratosphere (LOTUS) multiple linear regression model (SPARC/IO3C/GAW, 2019), we found that the stratospheric ozone concentrations at Uccle declined at a significant rate of around 2%/decade since 1969, rather consistently over the different stratospheric levels. This overall decrease can mainly be assigned to the 1969-1996 period with a rather consistent decline rate around -4%/decade. Since 2000, a recovery between
25 +1 to +3%/decade of the stratospheric ozone levels above Uccle is observed, although not significant and not for the upper stratospheric levels measured by ozonesondes. Throughout the entire free troposphere, a very consistent increase of the ozone concentrations at 2 to 3 %/decade is measured since both 1969 and 1995, the latter trend being in almost perfect agreement with the trends derived from the In-service Aircraft for a Global Observing System (IAGOS) ascent/descent profiles at Frankfurt. As the amount of tropopause folding events in the Uccle time series increased significantly over time,
30 increased stratosphere-to-troposphere transport of recovering stratospheric ozone might partly explain these increasing tropospheric ozone concentrations, despite the levelling off in (tropospheric) ozone precursor emissions and notwithstanding the continued increase of mean surface ozone concentrations. Furthermore, we illustrate the crucial role of ozonesonde



measurements for validation of satellite ozone profile retrievals. With the operational validation of Global Ozone Monitoring Experiment GOME-2, we show how the Uccle dataset can be used to evaluate the performance of a degradation correction
35 for the MetOp-A/GOME-2 UV sensors. In another example, we illustrate that the Microwave Limb Sounder (MLS) overpass ozone profiles in the stratosphere agree within $\pm 5\%$ with the Uccle ozone profiles between 10 and 70 hPa. Another instrument on the same AURA satellite platform, Tropospheric Emission Spectrometer (TES), is generally positively biased with respect to the Uccle ozonesondes in the troposphere by up to ~ 10 ppbv, corresponding to relative differences up to $\sim 15\%$. Using the Uccle ozonesonde time series as reference, we also demonstrate that the temporal stability of those last two
40 satellite retrievals is excellent.

1 Introduction

Ozone, O_3 , is a key trace gas in the Earth's atmosphere, where it mainly resides between the surface and the top of the stratosphere (about 50 km). Ozone is mainly produced in the tropical stratosphere and transported to the lower stratosphere at high latitudes. Depending on its altitude, ozone is involved in different chemical reactions and therefore has a different
45 impact on life on Earth. Stratospheric ozone absorbs the harmful solar ultraviolet (UV) radiation, hereby protecting life on Earth, and warming the stratosphere. This protective shield has been in danger due to anthropogenic emissions of ozone depleting substances (ODSs, such as chlorofluorocarbons or CFCs) since the 1970s, with the Antarctic springtime ozone hole as the most striking signature. Thanks to the Montreal Protocol (1987, and subsequent amendments and adjustments), positive trends in the ozone concentrations in the upper stratosphere are observed since 2000 (SPARC/IO3C/GAW, 2019).
50 Ozone is also an important absorber of infrared (terrestrial) radiation, mainly in the tropopause region, and therefore acts as a greenhouse gas, estimated to be responsible for 1/4 to 1/3 of the Earth's warming over the past 200 years (Thompson et al., 2019). Tropospheric ozone is also the main source of the OH free radical, the primary oxidant in the atmosphere, responsible for removing many compounds (including atmospheric pollutants) from tropospheric air. At the surface, ozone is an air pollutant that adversely affects human health, natural vegetation, and crop yield and quality (e.g. Cooper et al., 2014).
55 Because of the many roles of ozone, the knowledge and measurement of the vertical distribution of the ozone concentration in the atmosphere – and its variability in time – is crucial. Vertical ozone profiles can be obtained from ground-based instruments (Dobson/Brewer Umkehr, lidar, FTIR, and microwave radiometer), balloon-borne techniques (ozonesondes), and satellite-based measurements (using solar/stellar occultation, limb emission/scattering and nadir-viewing techniques) (see Hassler et al., 2014 for details).
60 In this research, we focus on ozonesondes, lightweight and compact balloon-borne instruments measuring the ozone concentration from the surface through the mid-stratosphere (about 10 hPa or 30 km). In electrochemical ozonesondes atmospheric ozone is measured via an electrochemical reaction of ambient air bubbling in a solution of potassium iodide (KI), by means of a stable miniature pump. In a Brewer-Mast sonde two electrodes are immersed in a buffered KI solution (Brewer and Milford, 1960), while ECC sondes consists of two half cells with different solutions of KI (Komhyr, 1969). The



65 ozonesonde is launched in tandem with a radiosonde that also transmits air pressure, temperature, humidity and wind data to a ground station. With a 20-30s response time of the ozone cells and an ascent rate of about 6 m/s, the effective vertical resolution of the ozone signal lies nowadays around 150 m.

Regular measurements with ozonesondes started in the second half of the 1960s at a few sites: in 1966 at Resolute Bay (Canada), in 1967 at Hohenpeissenberg (Germany), in 1968 at Payerne (Switzerland), in 1969 at Uccle (Belgium), and in
70 1970 at Wallops Island (USA). These ozone sounding stations provide the longest time series of vertical ozone distribution. Up to an altitude of about 30 km, ozonesondes constitute the most important data source with long-term data coverage for the derivation of ozone trends with sufficient vertical resolution, particularly in the climate sensitive altitude region around the tropopause. Furthermore, ozonesondes are widely used to study photochemical and dynamical processes in the atmosphere or to validate and evaluate satellite observations and their long term stability (Smit and ASOPOS panel, 2014,
75 and references therein).

In this paper, we focus on the ozonesonde measurements at Uccle, covering 50 years, demonstrating its scientific relevance and the major achievements. Ozonesondes are still the only technique able to measure the ozone concentrations from the surface all the way up to the middle stratosphere with very high (absolute) accuracy and vertical resolution. Therefore, they have many application areas in which they are crucial: (i) quantifying the long-term variability in stratospheric and
80 tropospheric ozone, (ii) as backbone for satellite validation, with satellites mostly measuring ozone only in stratosphere or upper troposphere, and (iii) for process studies in stratospheric-tropospheric exchange, and chemical production/destruction of ozone. The strength and uniqueness of the ozonesonde measurements, and in particular of our long-term and very dense Uccle dataset, lie in combining all those different aspects of ozone research. In this paper, we will first give a description of the ozonesonde measurements at Uccle from a historical point of view (Sect. 2) and describe briefly which data processing
85 has been applied to the ozonesonde measurements used in this paper (Sect. 3). In Section 4, we assess the time evolution of ozone at Uccle at different vertical layers against the background of recent findings in ozone variability. The fifth section illustrates the important role of the Uccle data for the validation of satellite ozone retrievals. Finally, in Section 6, concluding remarks and perspectives are given.

2 The Uccle ozone measurements: a historical overview

90 In this section, we give a brief overview of the history of the ozone measurements at Uccle (Brussels, Belgium, 50°48'N, 4°21'E, 100 m asl). We explain why the ozone sounding program has been initiated more than 50 years ago and discuss the presence of a period of gaps in the time series (Sect 2.1). We also describe which efforts have been taken during this time period to guarantee the homogeneity of the time series of ozonesondes between ascent and descent profiles (Sect. 2.2.1), with changing environmental conditions (Sect. 2.2.2), and between different ozonesonde types (Sect. 2.2.3).



95 **2.1 The start of the ozone observations**

The ozone sounding program at the Royal Meteorological Institute of Belgium (RMI) at Uccle was initiated by Prof. Jacques Van Mieghem, director of RMI from 1962 to 1970. Initially the ozone soundings were not performed out of a concern for possible human influence on the ozone layer, but rather to use ozone as a tracer to study the general air circulation in the troposphere and the lower stratosphere. Therefore, from the beginning it was planned to perform regular ozone soundings
100 three times per week (on Monday, Wednesday and Friday).

In 1965 and 1966 the first few soundings were performed with Regener chemiluminescent ozonesondes. A well-known effect of this sonde type is that it shows changes in sensitivity during the ascent trajectory (see e.g. Hering and Dütsch, 1965). For that reason it was decided to switch to Brewer-Mast electrochemical ozonesondes (developed by Brewer and Milford (1960) and commercially produced by the Mast Development Company at Iowa, USA) at RMI from November
105 1966 onwards. Based on a number of criteria such as continuity of the measurements and how well the preparation of the sondes was documented, it was decided to use the ozone soundings for scientific studies only from 1969 onwards, when Dirk De Muer took over the ozone research at RMI (in July 1969).

In the period from February 1983 to January 1985 there were only a few ozone soundings. This gap in our time series was due to financial problems. Later on, when the Uccle time series of ozone soundings had proved its scientific value and with
110 the growing concern of a human influence on the ozone layer, the continuation of the soundings became less an issue. In the course of time different radio sounding systems have been used. A major change occurred in 1990 when digital data transmission at high sampling rate was introduced, which allowed a higher vertical resolution of the profiles (not only at significant and standard pressure levels).

To normalize the integrated ozone amount of the ozone soundings, the Dobson spectrophotometer (no. 40, D40) at Uccle
115 was used since July 1971; before that date an interpolation of values from other Dobson stations in the European network was employed. In 1984, the Uccle site was equipped with a single Brewer UV spectrophotometer (no. 16), and with a double Brewer instrument (no. 178) in September 2001, to provide total ozone column measurements.

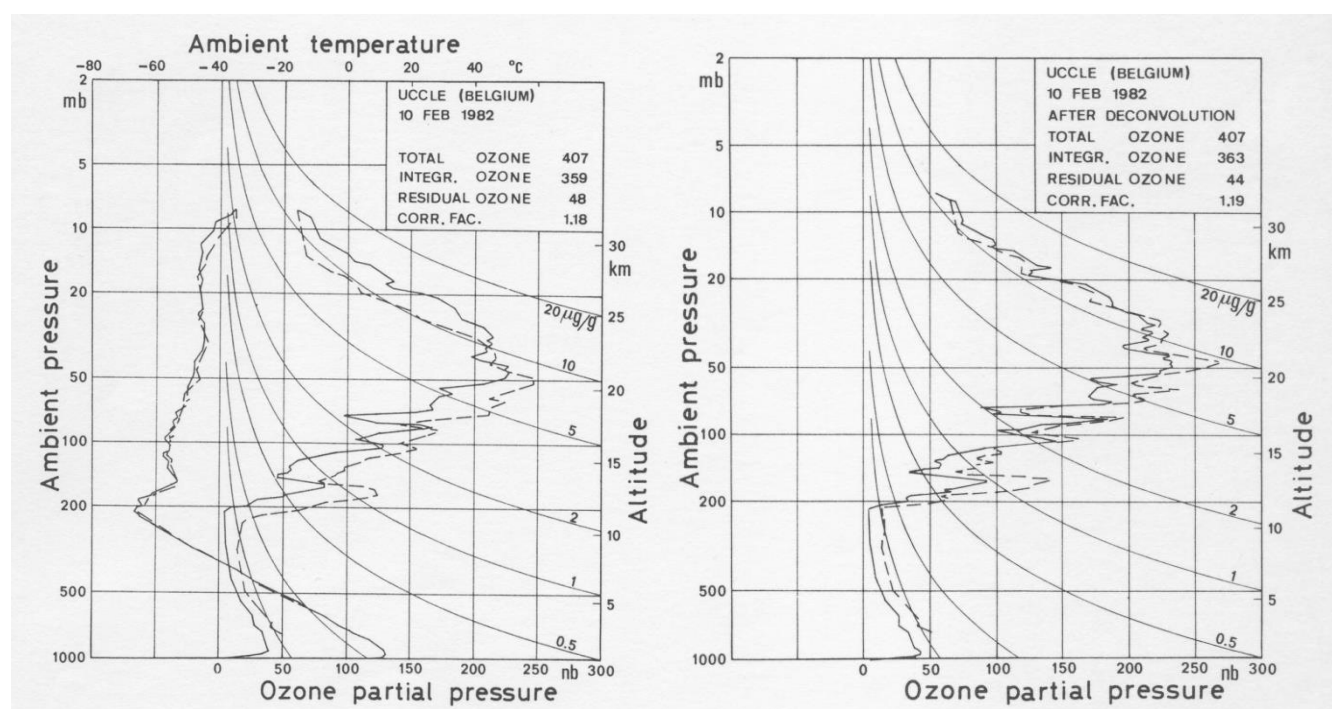
2.2 Challenges

2.2.1 Frequency response of the electrochemical ozonesonde

120 In 1970 the ozone sounding program was adapted to gather also the data during the descent of the sonde after balloon burst. De Muer (1981) found that the measured ozone concentrations in the lower stratosphere and the troposphere were systematically higher during the descent than during the ascent. As possible explanation a contamination of the ozonesonde at the ascent (e.g. by reducing constituents in the atmospheric boundary layer) and/or the response time of the sensor were mentioned. Therefore, De Muer and Malcorps (1984) analysed the frequency response of the combined ozone sensor and air
125 sampling system of Brewer-Mast ozonesondes by means of a Fourier analysis. They concluded that the measured frequency response can be represented by a first-order process and a diffusion process in series. A study of the dependency of the



130 global transfer function of the sensor system as a whole on solution temperature and on background ozone level provided better insight into the performance of electrochemical ozonesonde, so that a method for deconvolution of the ozone profiles through a process of Fast Fourier transform could be developed. An example of an ozone profile before and after deconvolution is shown in Figure 1. After deconvolution the observed ozone values during the descent are still larger than the ascent values in the troposphere and the lowest layers in the stratosphere, which was then attributed to the effect of SO₂ on the ozonesonde measurements in the boundary layer.



135 **Figure 1: Ozone sounding at Uccle on 10 February 1982 with a Brewer-Mast ozonesonde before (left) and after (right) deconvolution of the ozone profile for both ascent (solid line) and descent (dashed line) of the sonde. In the left panel, the vertical profile of the air temperature is also shown (figure taken from De Muer & Malcorps, 1984).**

2.2.2 The impact of the boundary layer SO₂ concentrations on the ozone measurements

140 As SO₂ has even stronger absorption bands than ozone in the UV 305-340 nm wavelength range used for the total ozone determination with a Dobson spectrophotometer, total ozone amounts might be overestimated with this instrument in case of a considerable total vertical SO₂ column amount, as discussed by Komhyr and Evans (1980). In the suburban area of Uccle, the SO₂ densities near the ground were quite elevated at the start of the ozone measurements, but showed a steep decrease from the late 1960s to the early 1990s (Fig. S1). A comparison between quasi-simultaneous total ozone observations at Uccle
145 with a Dobson and a Brewer spectrophotometer showed that there was no drift in the difference between the two datasets if



the effect of SO₂ was taken into account (De Backer and De Muer, 1991). It was also found that the SO₂ correction of the Dobson spectrophotometer D40 data had a significant effect on the calculated total ozone trend (De Muer and De Backer, 1992), and made this trend consistent with the one derived from reprocessed Total Ozone Mapping Spectrometer (TOMS) satellite data for a sub-period in which both datasets were available.

150 Ozonesonde measurements by the KI method are sensitive to interference by oxidizing or reducing agents (e.g. Tarasick et al., 2020, and references therein). In particular, SO₂ can cause an important reduction in the ozone detected of 100%, and excess SO₂ can accumulate in the cathode solution, affecting ozonesonde measurements well above the polluted boundary layer (Komhyr, 1969, De Muer and De Backer, 1993, Morris et al., 2010), see also Fig. 1 and Fig. S2.

As a consequence, the variation of SO₂ density near the ground has a twofold effect on ozone soundings with electrochemical sondes: (i) the integrated ozone amount of the soundings is normalized by means of spectrophotometer data so that a trend in the latter data will lead to an effect on ozone trends from soundings, and (ii) due to the SO₂ interference with the ozonesonde cell reactions, any trend of SO₂ causes a distortion of ozone profile trends as a function of altitude. A method to calculate the vertical SO₂ distribution associated with each ozone sounding was developed, based on two assumptions: a constant SO₂ mixing ratio from the ground to the mixing layer height, and an exponentially decreasing mixing ratio above the mixing layer balancing the integrated SO₂ amount to the reduced thickness of the SO₂ layer (De Muer and De Backer, 1993). The effect of this correction for SO₂ interference on the vertical ozone trends in the 1969-1996 period is illustrated in Fig. S3.

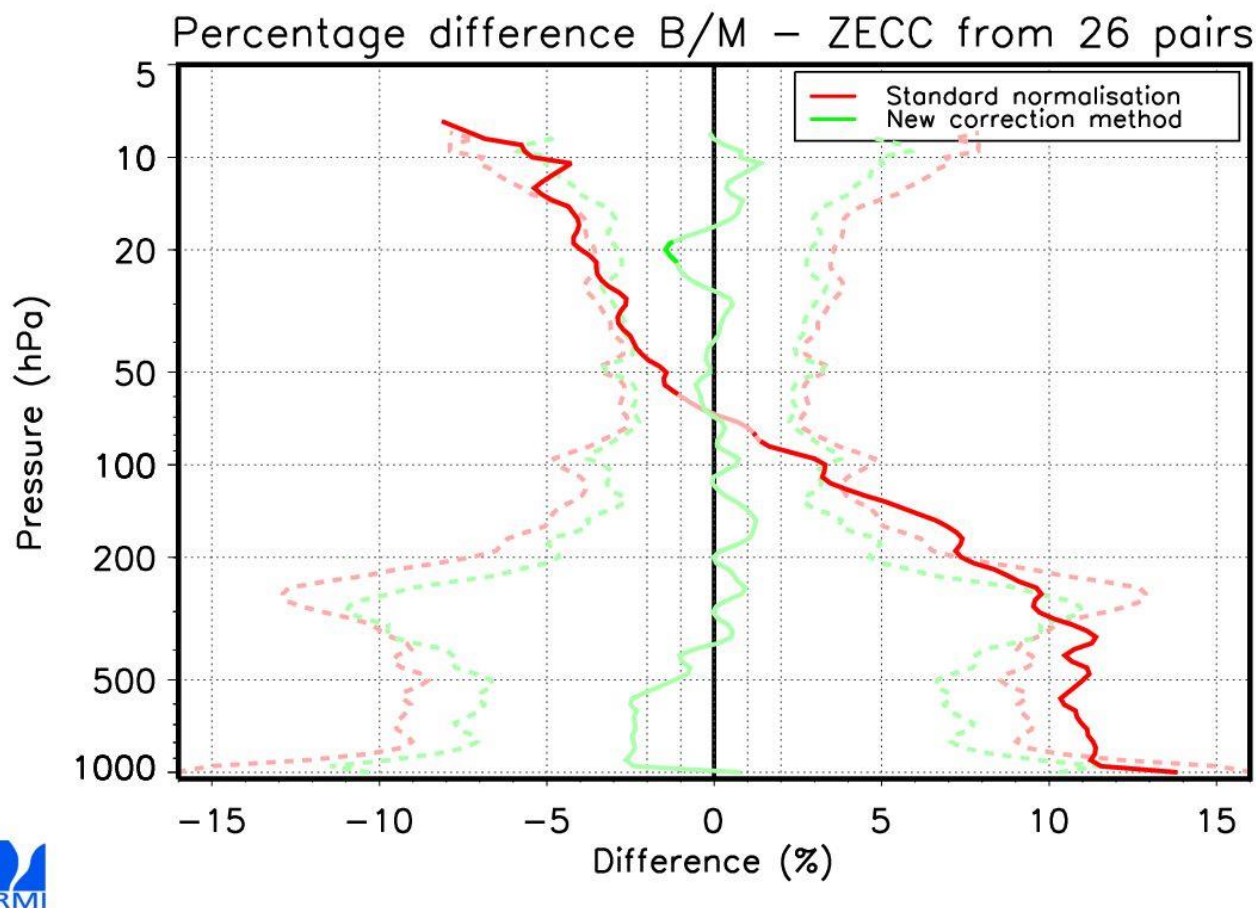
2.2.3 The transition from BM to ECC sondes

As mentioned before, at the start of the operational ozone sounding series the Brewer-Mast type of sensor was used. This type of ozonesonde had several issues at that time: (i) a strong reduction of the efficiency of the pump at low pressure (De Backer et al., 1998a), (ii) the loss of ozone in the sensor itself, causing a relatively high (up to 20%) underestimation of the integrated ozone from a sounding profile with respect to the total ozone measured with a Dobson or a Brewer spectrophotometer, and (iii) a variable response in the troposphere, depending on preparation (Tarasick et al., 2002).

Therefore, in the middle of the 1990s, RMI investigated the switch from the BM sondes to the ECC sensors (Komhyr, 1969), which seemed to perform better and were easier to prepare before launch. To document this transition, double soundings were launched about twice a month during one year. The comparison between both sensor types is shown in Fig 2. If standard correction methods for both sensors are used, large statistically significant differences appear: Brewer-Mast sensors overestimate tropospheric ozone and underestimate stratospheric ozone. De Backer et al. (1998a,b) developed a correction method (now called PRESTO, for PRESSure and Temperature dependent Total Ozone normalization, see Van Malderen et al., 2016) based on measurements of the pump efficiency in a pressure chamber and on a comparison with a calibrated ozone source and the total ozone column measured with a co-located ozone spectrophotometer. By applying this method, the differences are reduced below 3% almost throughout the whole profile and below the statistical significance level (see Fig.



- 2). The impact of this new pump correction method on the vertical ozone trends is also significant, especially for the 1969-1996 BM period (see Fig. S3 and Van Malderen et al., 2016).
- 180 Further validation of the method was done by comparing the profiles with measurements from the SAGE II satellite instrument (Lemoine and De Backer, 2001). This study showed that the PRESTO correction removed the jump, caused by the transition, in the time series at low pressures (compare Fig. 1 and 2 in Lemoine and De Backer, 2001).



- 185 **Figure 2:** Mean percentage differences between ozone profiles obtained with Brewer-Mast and (En-Sci model Z) ECC sensor during dual soundings with standard correction method (red) and with the PRESTO method (green). Thick lines denote the pressure levels where the differences between the mean profiles are statistically significant. The dashed lines are the one sigma variance of the distribution of the differences [fig. adapted from De Backer et al, 1998b].

3 The Uccle ozonesonde dataset

- 190 In this paper, the PRESTO correction has been applied to the entire ozonesonde dataset, i.e. to both the BM and ECC ozonesonde types, but with the appropriate different pump efficiency coefficients for the different types, to ensure



consistency over the entire data record of 50 years. Although a total ozone normalization is not required for the ECC sonde measurements (Smit and ASOPOS panel, 1994), it is applied for the entire Uccle time series within the PRESTO correction. To calculate the residual ozone above the balloon burst level, we use a combination of the constant mixing ratio approach and the climatological mean obtained from satellite ozone retrievals (McPeters and Labow, 2012). An alternative, homogenized, Uccle ozonesonde corrected dataset is available by request from the authors for the ECC time series since 1997 (Van Malderen et al., 2016), following the principles of the Ozonesonde Data Quality Assessment (O3S-DQA) activity (Smit et al., 2012), but is not used here to maintain the consistency over the entire time series. Differences between both versions of corrected Uccle ECC ozonesonde data, in comparison with nearby De Bilt (the Netherlands, 175 km north of Uccle), are highlighted in Van Malderen et al. (2016).

For the BM ozonesondes, the applied PRESTO corrections include (i) a correction for SO₂ interference on the ozone soundings (imperative to have reliable lower-tropospheric ozone trend estimates for the period 1969-1996, see Fig. S3), (ii) a correction for a negative background current caused by impurities in the sensor before October 1981, (iii) a correction for box temperatures depending on the insulating capacity of the Styrofoam boxes (a short discussion of those additional corrections and the proper references are given in the appendix A of Van Malderen et al., 2016), and (iv) an altitude correction for VIZ/Sippican radiosonde pressure measurements based on comparisons with wind-finding radar. Without this altitude correction (calculated sonde altitudes were too low), the calculated ozone concentrations with VIZ radiosondes were too low by 7.5 to 14%, depending on the manufacturing series of radiosondes (De Muer and De Backer, 1994). From 1990, the ozonesondes were combined at Uccle with Vaisala RS80 radiosondes, which showed a much smaller difference of the calculated altitude with respect to wind-finding radar data. Therefore, for the digital era period since 1990, no radiosonde pressure sensor bias corrections have been applied, although they have been identified in different studies (e.g. De Backer, 1999; Steinbrecht et al., 2008; Stauffer et al., 2014; Inai et al., 2015).

4 Temporal evolution of the vertical ozone concentrations at Uccle

As ozonesondes are the only devices that are able to measure ozone concentrations from the surface up to the middle stratosphere with high vertical resolution, they are very suitable to study and relate the temporal variability of ozone in different atmospheric layers. The evaluation of the temporal variability of the ozone measurements at Uccle is therefore organized in different sections. We first describe the total ozone temporal evolution (Sect. 4.1), continue with the stratospheric (Sect. 4.2) and tropospheric (Sect. 4.3) ozone trends, and we wrap up with the temporal behaviour of surface ozone and several ozone depleting substances (Sect. 4.4).

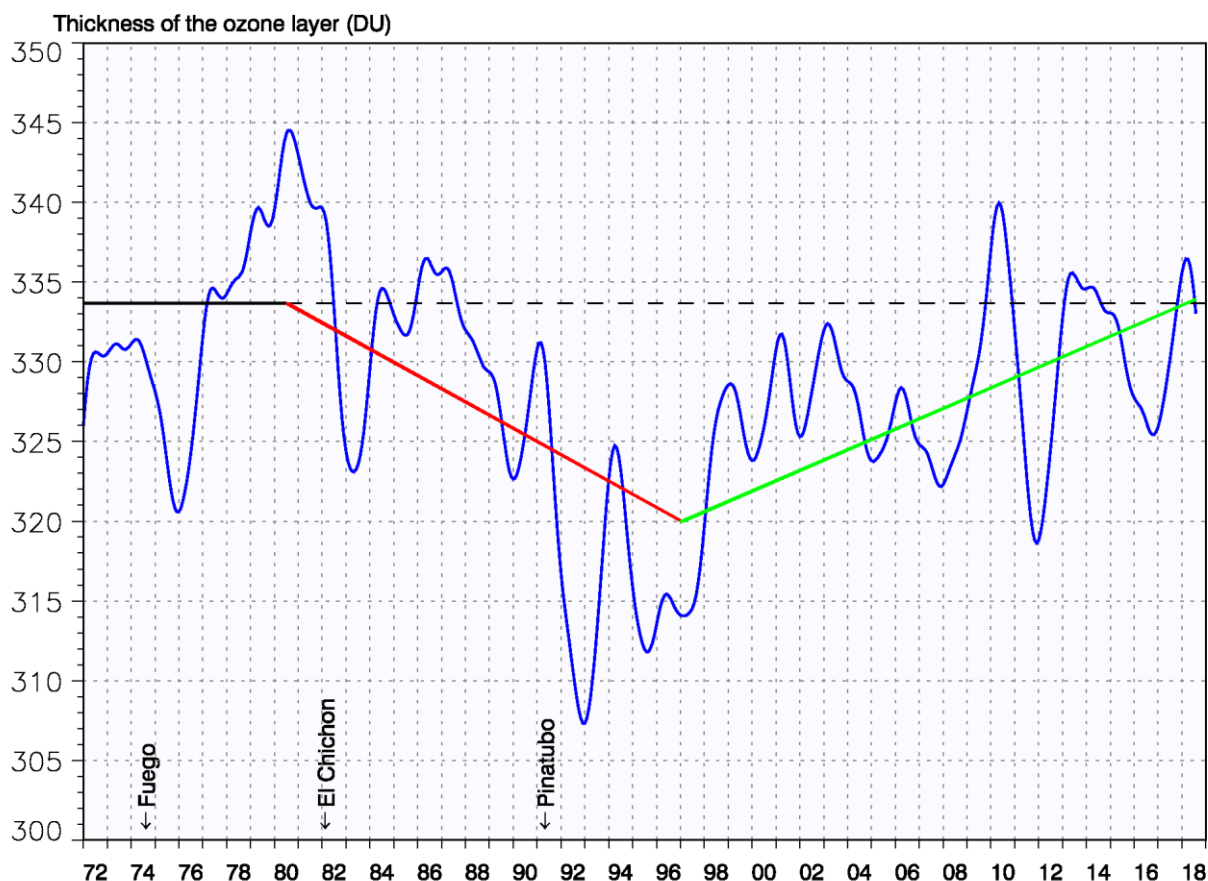
4.1 Total ozone trends

The total column ozone amounts at Uccle, available since 1971, are retrieved with a Dobson UV-spectrophotometer (no. 40, 1971-1989), a single Brewer UV spectrophotometer (no. 16, 1990-current, but used in the time series until the end of 2001),



and a double Brewer UV spectrophotometer (no. 178, 2002-current). The time series of total ozone measurements is shown in Fig. 3, but has been smoothed by applying a low-pass Gaussian filter with a width at half height of 12 months, to filter out variations with frequencies higher than one year. With this representation, the impact of the major (strato)volcanic eruptions of Fuego (Guatemala, Oct 1974), El Chichon (Mexico, Mar/Apr 1982), and Pinatubo (the Philippines, Jun 1991) on the Uccle total ozone concentrations pops up. Indeed, episodes of enhanced stratospheric aerosol-related ozone loss after those major volcanic eruptions (see e.g. Tie and Brasseur, 1995, Aquila et al., 2013 for a description of the mechanism behind) can clearly be identified in the time series. The inter-annual variability in Fig. 3 is very similar to the Northern Hemisphere (NH) annual mean total ozone time series of five bias corrected merged datasets in the 35–60° N latitude band in Weber et al. (2018; their Fig. 2). We refer to this paper for the discussion of several features (e.g. the excess total ozone in 2010, the 2011 and 2016 low ozone anomalies).

The long-term temporal variability of the total ozone amounts at Uccle is dominated by the 1980-1997 ozone decline (at a rate of 2.5%/decade) due to the anthropogenic production of ozone depleting substances (ODS), transported into the stratosphere, with peak concentrations in 1997. Subsequently, in the late 1990s, the annual mean total ozone started to increase again (at a rate of 2%/decade at Uccle for the period 1997-2018). This increase was due to the combination of the slow decrease in ODSs and of atmospheric dynamics, notably ozone transport via the Brewer–Dobson circulation, causing also the interannual variability described in Weber et al. (2018). It should also be noted that the strongest increase of the total ozone amounts since the beginning of this century took place in Uccle in late winter – early spring (Feb-Apr), at a rate of 3-4%/decade, while the ozone transport by the Brewer-Dobson circulation from its tropical source region poleward and downward into the lower stratosphere is strongest during wintertime (e.g. Butchart, 2014; Langematz, 2019).



245 **Figure 3: Evolution of the total ozone column at Uccle as observed with Dobson D40 (1972-1989), Brewer 16 (1990-2001), and Brewer 178 (2002-present). Linear trends during the periods 1980-1997 and 1997-2018 are shown respectively in red and green. The horizontal black full line marks the 1972-1980 total ozone average, extended until the end of the time series by the dashed horizontal line. The periods of major volcanic eruptions affecting the ozone layer are indicated on the time axis as well.**

4.2 Stratospheric ozone trends

For calculating the vertical distribution of trends in the stratospheric ozone concentrations from the Uccle ozonesonde data, we use the altitude relative to the tropopause height as the vertical coordinate. The tropopause applied here is the standard
250 (first) thermal tropopause (WMO, 1957), and is derived from the vertical temperature profiles measured by the Uccle radiosondes, as described in Van Malderen and De Backer (2010). The implemented statistical model to calculate trends is the Long-term Ozone Trends and Uncertainties in the Stratosphere (LOTUS) multiple linear regression model (SPARC/IO3C/GAW, 2019). This model uses an independent linear trend (ILT) method as a trend term, which is based on
255 two different, independent, trends to describe the ozone decrease until 1997 (ODS increase) and the slow ozone increase since the early 2000s (after the turnaround in ODS concentrations). These two periods have been used since WMO (2014)



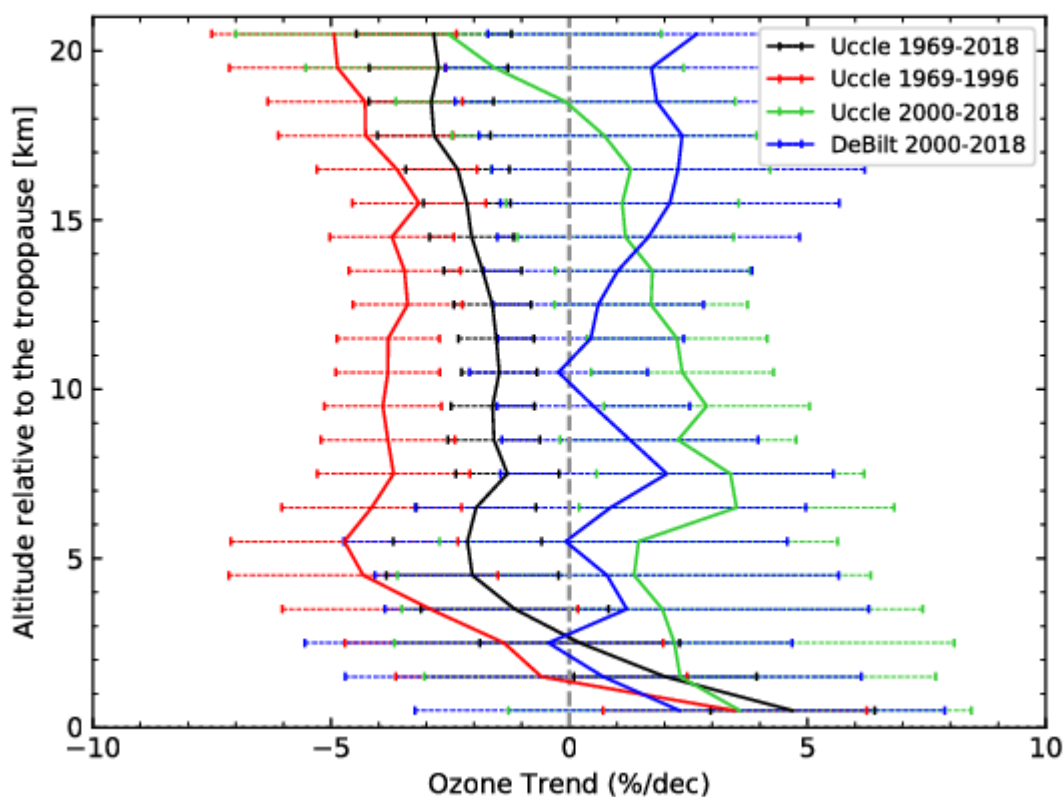
and their use avoids endpoint anomalies near the turnaround in 1997 for the two independent linear trend terms in the ILT method. Additionally, the LOTUS regression includes two orthogonal components of the quasi biennial oscillation (QBO), the 10.7 cm solar radio flux, El Niño Southern Oscillation (ENSO) without any lag applied, and the Aerosol Optical Depth (AOD, extended past 2012 by repeating the final available value from 2012 as the background AOD). Four Fourier components representing the seasonal cycle are also included. The final choice of those proxies (and possible lags) in LOTUS was based on retaining the optimal regression for global analysis of satellite data and broad latitude band analyses. Therefore, proxies describing rather local or small-scale phenomena might not have been included in the general "LOTUS regression" model. In particular, using an alternative stepwise multiple linear regression model for the Uccle stratospheric ozone amount, we found that the Uccle tropopause pressure and the Arctic Oscillation are significant proxies as well (contributing statistically significant, i.e. at the 95% significance level of the *t*-test, to the regression coefficient). However, here, the analysis is limited to the LOTUS model.

The vertical profile of stratospheric ozone trends is shown in Fig. 4. From 1969 to 1997, stratospheric ozone concentrations decrease almost uniformly (and significantly) at a rate around -4 %/decade, except at the layers just above the tropopause. Since 2000, the stratospheric ozone concentrations increase with about 2 %/decade, but only significantly at the layers below and at the ozone maximum (from 6 to 13 km above the tropopause, or 17 to 24 km for an average tropopause height of 11 km at Uccle). The insignificant negative trend of the Uccle ozone concentrations at the upper levels of Fig. 4 should be treated with caution, as the reliability of the ozonesonde instrument at those levels (above 30 km) is reduced. This is due to the increasing uncertainty in the pump efficiency at low pressures, the different stoichiometry of the chemical reaction due to a reduced amount of sensing solutions, frozen solutions, etc. Additionally, an increase of the burst altitude in the Uccle ozonesonde time series in recent years and inhomogeneities due to changing pressure sensors with different radiosonde types might have an impact on the ozone trends at these very low pressures. In fact, the negative ozone trends are also less pronounced if calculated for absolute altitude levels. When we compare the post 2000 trends with those from the ozonesondes launched at De Bilt, the overall stratospheric positive insignificant trends apply for both stations, also at the higher altitude levels at De Bilt. The larger trend uncertainties for the De Bilt time series can be explained by the smaller frequency of launches (once a week versus three times a week at Uccle).

Both the Uccle and De Bilt time series do not show a significant decline in lower stratospheric (13-24 km) ozone amounts, as reported by Ball et al. (2018, 2019) for the periods 1998-2016 and 1998-2018 respectively, from multiple (merged) satellite measurements in the lower stratosphere between 60°N and 60°S. Using the Modern-Era Retrospective Analysis for Research and Applications Version 2 (MERRA-2) ozone output fields, Wargan et al. (2018) found a discernible negative trend of -1.67 ± 0.54 Dobson units per decade (DU/decade) in the 10-km layer above the tropopause between 20°N and 60°N. Also the latest Scientific Assessment of Ozone Depletion (WMO, 2018), largely based on the LOTUS final report (SPARC/IO3C/GAW, 2019), concluded that "there is some evidence for a decrease in lower stratospheric ozone from 2000 to 2016", although not statistically significant in most analyses. This decline, contradictory to the decline of ozone-depleting substances since 1997, is attributed to changes driven by dynamical variations (Chipperfield et al., 2018), in the form of



290 enhanced isentropic mixing between the tropical (20°S–20°N) and extratropical lower stratosphere in the past two decades
(Wargan et al., 2018). However, although never significant, we found that the positive Uccle ozone trends in the lower
stratosphere are rather robust, independent of the starting date (1997/1998/2000), the used vertical coordinate system
(absolute or relative to the tropopause), and the trend model used (LOTUS MLR or simple linear fit). The lower
stratospheric ozone trends derived from the De Bilt time series show a larger variability between positive and negative
295 statistically insignificant values, especially in the ten lowest kilometres.



300 **Figure 4:** Vertical distribution of trends of stratospheric ozone concentrations at Uccle for different periods (see text) and at De
Bilt (2000-2018). The trends and their uncertainties are calculated with the LOTUS multiple linear regression model (see text and
SPARC/IO3C/GAW, 2019), including an independent linear trend term. The 2-sigma error bars represent the trend uncertainty
305 estimated by the regression model (using the fit residuals). For the Uccle 1969-2018 time series only, one linear trend term is
included in the model instead.

To understand the differences in the lower-stratospheric ozone trends since the end of the nineties, we also consider the
temperature trends in the stratosphere here (see Fig. S4), as the evolution of stratospheric ozone in a changing climate also
depends on the cooling of the stratosphere due to increases in greenhouse gases (GHGs). Before 1997, the stratosphere
305 cooled significantly by -0.9 to -0.5 °C/decade, corresponding with both the tropospheric warming due to the increase of



GHGs and the decreasing stratospheric ozone concentrations (Philipona et al., 2018). After 2000, the stratospheric cooling at both Uccle and De Bilt ceased at the altitudes where ozone concentrations peak and where their radiative impact on stratospheric temperatures is largest. This stratospheric warming is however not significant. Above and below the ozone maximum, the sign of trends between Uccle (respectively positive and negative) and De Bilt (respectively negative and positive) are reversed. As such, there is no clear similar covarying behaviour between ozone and temperature changes in the lower stratosphere at these two sites. However, when averaging the Payerne, Hohenpeissenberg and Uccle ozonesonde measurements, Philipona et al. (2018) found very similar seasonal and annual changes for temperature and ozone. With the exception of the fall season, annual and seasonal profiles switch from negative to positive trends before and after the turn of the century, for both ozone and temperature.

Finally, as we use the altitude relative to the tropopause as vertical coordinate, we should also mention the time variability of the tropopause height here. The tropopause height is increasing at both Uccle and De Bilt for all considered periods, but with different magnitudes: for Uccle, these are 6.98 ± 1.12 m/decade (1969-2018), 13.81 ± 3.00 m/decade (1969-1996), and 11.62 ± 79.42 m/decade (2000-2018), while for De Bilt the post-2000 trend magnitude is 25.73 ± 19.23 m/decade. These increases in tropopause altitudes are consistent with results from the global study in Xian and Homeyer (2019) based on radiosondes and reanalyses, although with smaller magnitudes (they found increases of 40–120 m per decade for the period 1981-2015). With climate model experiments, Santer et al. (2003) ascribed the simulated rise in tropopause altitude over 1979–1999 to cooling of the stratosphere (caused by ozone depletion) and warming of the troposphere (caused by well-mixed greenhouse gases).

We can conclude here that the Uccle stratospheric ozone trends before 1997 are well understood, but that the behaviour after 2000 is harder to explain due to its interaction with stratospheric temperature and tropopause variability, hence due to dynamics, induced by increasing GHG concentrations.

4.3 Tropospheric ozone trends

Ozone in the troposphere is affected by many processes. Stratosphere-troposphere inflow and photochemical formation by interaction with sun light and ozone precursors (NO_x , CO and Volatile Organic Compounds) increase the ozone levels, while photochemical destruction of ozone in low NO_x conditions (e.g. marine boundary layer and free troposphere, through OH- HO_2 cycle) or at high NO_x concentrations (urban regions under titration, i.e. via reaction with NO), and dry deposition on the ground removes ozone from the troposphere. Its short lifetime causes highly variable ozone concentrations in space and time, which complicates the understanding of the processes at play at all relevant spatio-temporal scales (Young et al., 2018). Moreover, the production of ozone in the troposphere is sensitive to variations in air temperature, radiation and other climatic factors (Monks et al., 2015).

Tropospheric ozone is measured with ozonesondes, by commercial aircraft, with different types of ground-based remote sensing instruments and with satellite instruments. Besides clear regional differences, the distribution and trends of ozone in the troposphere are not always consistent between these different datasets, and even not between different retrieval methods of the same satellite (e.g. Cooper et al., 2014, Gaudel et al., 2018). In fact, measuring the vertical profile of tropospheric



340 ozone concentrations from satellites remains very challenging and relies on ground-based retrievals of ozone for validation (see Sect. 5).

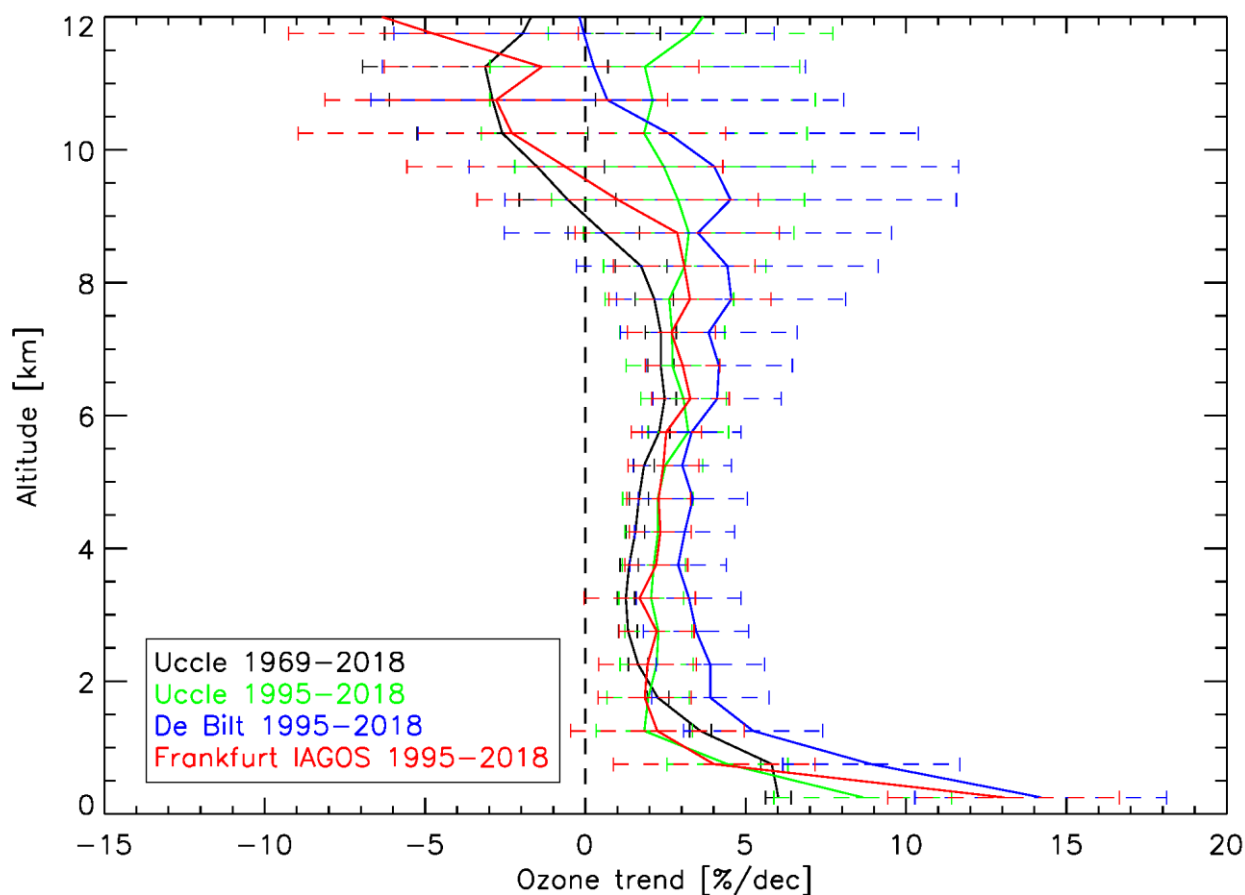


Figure 5: Vertical distribution of trends of tropospheric ozone concentrations at Uccle for different periods, at De Bilt (ozonesonde data) and Frankfurt (IAGOS data) for 1995-2018. Simple linear trends are calculated for monthly ozone anomalies in 1 km altitude ranges and the error bars are the 2σ standard deviations.

345 Here, we calculated the tropospheric ozone trends from the Uccle and De Bilt ozonesonde time series and the MOZAIC
(Measurement of Ozone and Water Vapour by Airbus in-service Aircraft) and IAGOS (In-service Aircraft for a Global
Observing System) ascent and descent profiles at Frankfurt airport, at about 320 km from Uccle. This MOZAIC-IAGOS
dataset consists of more than 27600 profiles, starting in August 1994, and is combined with the data from Munich airport,
approximately 300 km southeast of Frankfurt, between 2002 and 2005 (about 4200 flights), to fill a large data gap in 2005
350 (also done in e.g. Petetin et al., 2016). We used simple linear trends based on the monthly anomalies at different altitude
levels (see Fig. 5) for the period 1995-2018, as there is no consensus on the used proxies to account for natural variability in
a multiple linear regression model as for stratospheric ozone (e.g. LOTUS). First, the extremely good agreement between the



Uccle and IAGOS vertical ozone trends in the free troposphere (3-8 km) for the 1995-2018 period is striking. Although the integrated tropospheric ozone amounts for this altitude range are lower for the region above Frankfurt (14.9 DU) than above
355 Uccle (16.2 DU), the overall relative trends are similar (resp. 2.09 ± 1.01 %/decade and 2.47 ± 1.01 %/decade, see Fig. S5). The De Bilt trends are larger in the free troposphere, with also larger uncertainties probably due to the lower launch frequency. Note also the sensitivity analysis of IAGOS profiles above Europe by Chang et al. (2020), who determined that an optimal sample frequency of 14 profiles per month is required to calculate trends with their integrated fit method (and about 18 profiles a month when this method is not used). Near the surface, the De Bilt trend is in better agreement with the
360 Frankfurt trend, but the local surface ozone production and destruction and the boundary layer dynamics can vary substantially between the three sites considered here. In the upper troposphere, the ozone concentration trends deviate more between the different datasets, both in magnitude and sign, with larger trend uncertainties. At these altitudes, the aircraft could be very distant from Frankfurt (or Munich) airport, as the ascent/descent profiles stop/start at about 400 to 500 km from the airport. The measurements at these altitudes are hence representing large areas. Therefore, the closer agreement
365 between the Uccle and De Bilt trends above 8 km compared to the IAGOS trend might be ascribed as well to a similar source region.

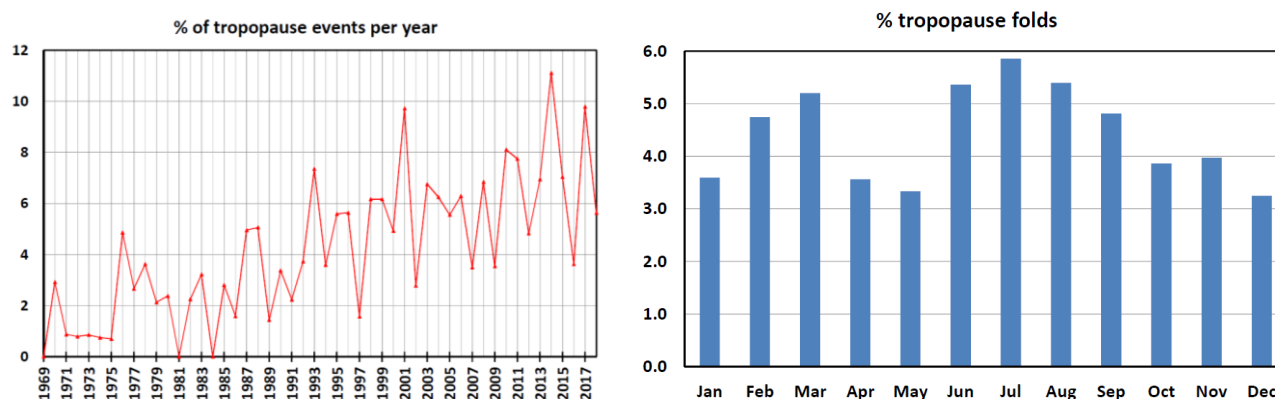
The Uccle tropospheric ozone concentrations have been increasing at about the same rate since 1969 as in the most recent considered period here (since 1995, but the post-2000 trends have the same magnitude). The increase in (free) tropospheric ozone concentrations above Uccle until the early 2000s is consistent with the findings reported above (Western) Europe in
370 the literature review of Cooper et al. (2014). Over the 2000-2014 period, the emissions of the key ozone precursor, nitrogen oxides (NO_x), decline in North America and Europe due to transportation and energy transformation (Hoesly et al., 2018). Therefore, the overall increase in ozone concentrations has flattened, but resulted in spatially and seasonally varying tropospheric ozone trends over North America and Europe, without consistency in even the sign of the ozone trends (Gaudel et al., 2018, and references therein). However, Cooper et al. (2020) concluded, based on the IAGOS observations, that the
375 Western Europe free tropospheric trends since 1995 are predominantly positive. Using a different statistical approach, i.e. a nonlinear regression fit of a quadratic polynomial fit to normalized, deseasonalized monthly mean ozonesonde (merged data from Uccle, Hohenpeissenberg, and Payerne) and MOZAIC/IAGOS data (Frankfurt) between 3 to 4 km altitude, Parrish et al. (2020) indicated that those ozone concentrations increased through the 1990s, reached a maximum in the years 2001 (merged ozonesonde) and 2007 (IAGOS) and have since then decreased.

To explain the tropospheric ozone concentration trends, Griffiths et al. (2020) used a chemistry-climate model employing a stratosphere-troposphere chemistry scheme, and found that for the period 1994-2010, despite a levelling off in emissions, increased stratosphere-to-troposphere transport of recovering stratospheric ozone drives a small increase in the tropospheric ozone burden. Taking advantage of the high vertical resolution of the ozone profiles and the high frequency of launches at Uccle, we focus on the time variability of specific cases of deep intrusions of stratospheric air into the troposphere, i.e.
385 tropopause folds. These occur because of the ageostrophic circulation at the jet entrance and coincide with the frontal zone beneath the jet. The algorithm applied in this work detects tropopause folds in the Uccle ozone sounding profiles as ozone



rich, stable and dry air mass layers located in an upper level front in the vicinity of an upper tropospheric jet stream, and is described in Van Haver et al. (1996). This identification is also illustrated by means of an example of an ozone sounding in Fig. S6.

390 Tropopause folds are rather rare events at Uccle: out of the 6526 soundings analysed for the 50 year period (1969-2018), only 290 soundings (or 4.4%) showed evidence of a tropopause folding. However, similar occurrence rates (between 3 and 10%) have been found over Europe at French ozonesonde sites (Beekmann et al., 1997) and with other techniques (Rao et al., 2008, and Antonescu et al., 2013). On a monthly scale, most folding events occur in March, June, July and August (occurrence > 5%), whereas in January, April, May and December, the amount is lower (Fig. 6). What is most important here
395 within the context of the tropospheric ozone trends is the dramatic increase the amount of tropopause folding events over time with 0.14 ± 0.02 % per year (see also Fig. 6). Van Haver et al. (1996) detected a smaller and insignificant trend of 0.07 ± 0.11 % per year at Uccle for the 1969-1994 period. On one hand, the higher vertical resolution of the sounding data in the more recent digital era (since 1990) might have an impact on the larger detected number of tropopause folds, although the amount of events has continuously increased since then. On the other hand, climate change is expected to increase planetary
400 wave activity and so cause an accelerated Brewer-Dobson circulation. This projected acceleration, along with stratospheric ozone recovery, will lead to increased transport of ozone from the stratosphere into the troposphere and hence an expected higher rate of tropopause folding events (Tarasick et al., 2019, and references therein).



405 **Figure 6: Left: Relative frequency of detected tropopause folding events per year in the ozone soundings at Uccle. Right: Relative frequency of tropopause folding events per month.**

To conclude, we found very consistent positive vertical linear tropospheric ozone trends between Uccle, De Bilt, and Frankfurt (IAGOS) since 1995 (and even since 2000), which are consistent with other studies, both observational and from a modelling approach, but different processing and statistical methodologies can result in different European trend patterns for
410 the last two decades.



4.4 Surface ozone trends

In this section, we elaborate more on the trends in the time series of surface ozone and several ozone precursors measured in Uccle. As a matter of fact, the ozonesonde launch site at the urban background site Uccle also hosts surface measurements of ozone, NO, and NO₂, performed by the Brussels Environment Agency. CO measurements are available from a nearby urban traffic location at Elsene (< 5 km). From the surface measurements, we consider the (half-hourly averaged) values at 11h30 UT closest to the ozonesonde launch time. The monthly mean time series of those surface measurements are shown in Fig. 7 (monthly anomalies in Fig. S7), together with the lowest 1 km mean ozone measurements derived from the ozonesondes. The agreement between the surface ozone measurements from both devices is, in terms of monthly means, excellent, apart from a more or less constant offset. Both time series reveal a statistically significant (according to Spearman's test, see e.g. Lanzante, 1996) increase in surface ozone concentrations since 1986 (the onset of the surface ozone measurements at the Uccle site), with a trend value 25% higher for the surface ozone measurements compared to the sonde lowest 1 km measurements (0.47 vs. 0.38 $\mu\text{g m}^{-3} \text{ yr}^{-1}$ in absolute terms). Uccle is a suburban site, so, its increase in mean surface ozone concentrations is in line with the findings from Yan et al. (2018) over European suburban and urban stations during 1995–2012¹, with trends between 0.20–0.59 $\mu\text{g m}^{-3} \text{ yr}^{-1}$. For the 1995-2018 time period, the ozonesonde trend (0.41 $\mu\text{g m}^{-3} \text{ yr}^{-1}$, see also green curve in Fig. 5 for relative trend) is more elevated than the surface ozone trend (0.28 $\mu\text{g m}^{-3} \text{ yr}^{-1}$ or 6.4±2.9 %/decade), and both are statistically significant. This former ozonesonde trend estimate equals the value for the entire ozonesonde time series 1969-2018 (0.39 ± 0.07 $\mu\text{g m}^{-3} \text{ yr}^{-1}$), as was the case for the entire tropospheric ozone trends (see again Fig. 5).

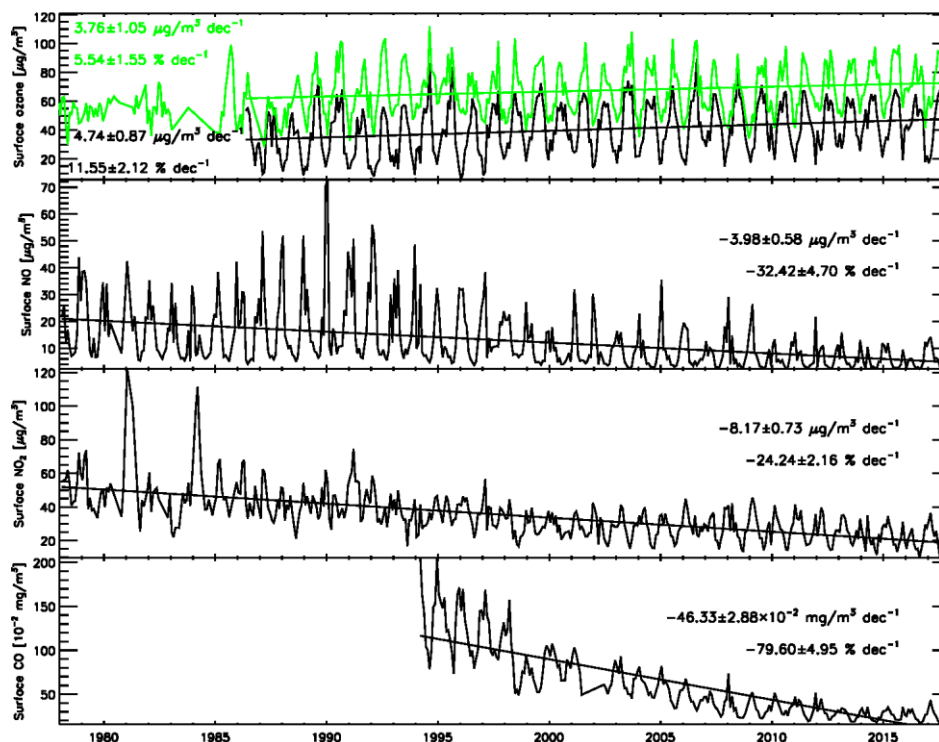
We now compare the surface ozone trends with the trends of the ozone precursor concentrations measured at or near the Uccle site (NO, NO₂, and CO, see Fig. 7, and monthly anomalies in Fig. S7). Apparently, there seems to be a mismatch between the increase in ozone concentrations and the strong decreases of all available measured ozone precursor concentrations, also noted in other studies (e.g. Tørseth et al., 2012; Lefohn et al., 2018). However, different aspects should be taken into consideration here. First, the photochemical production of tropospheric ozone also involves reactions implying volatile organic compounds (VOCs) and hydroxyl radical oxidation of methane and non-methane hydrocarbons, in the presence of nitrogen oxides (Monks et al., 2015). In NO_x limited conditions (i.e. rural locations or downwind of urban plumes and major point sources and at times of high photochemical activity on hot sunny summer days), increases in NO_x emissions lead to ozone increases while increases in VOC emissions may have limited impacts. In VOC or radical-limited conditions (in areas with large NO_x emissions such as urban core areas and power plant plumes, and under conditions of lower photochemical activity like night-time hours, cloudy days, wintertime days), increases in NO_x emissions may lead to localized ozone decreases, while increases in VOC emissions result in ozone increases (Lefohn et al., 2018 and references therein). Unfortunately, VOC measurements are not available at the Uccle surface site. Secondly, although tropospheric

¹ For comparison, over the same period, the Uccle surface ozone trend is 0.37 ± 0.20 $\mu\text{g m}^{-3} \text{ yr}^{-1}$, but only 0.07 ± 0.23 $\mu\text{g m}^{-3} \text{ yr}^{-1}$ for the ozonesonde measurements.



ozone is mainly produced from the photolysis of NO_2 , NO destroys ozone especially during night-time, implying that reductions in NO_x emissions might adversely result in more ozone, especially in highly polluted areas such as cities (Yan et al., 2018). Chang et al. (2017) also noted that in Europe, the NO_2 column amount tends to be negatively correlated with
445 ozone in urban sites. Moreover, they mention that in the warm season NO_x emissions tend to produce ozone, while in the cold season fresh emissions tend to destroy ozone in urban areas, which is also observed on a European scale (Tørseth et al., 2012). For Uccle, however, we do not find substantial differences between summertime and wintertime ozone trends in both datasets. Furthermore, the ozone trends also depend heavily on the chosen ozone metric (Lefohn et al., 2018). Here, we used the monthly means of the 11h30 UTC values, because the ozonesondes are launched around this time, with a very limited
450 frequency for surface ozone measurements (hence the need for monthly means). However, the large NO_x emission reductions that have occurred in the past several decades in the European Union (EU) have led to a compression of the ozone distribution, where the high levels shift downward (reduced ozone peak concentrations) and the low levels shift upward (increase in the ozone baseline level), as noted and explained by e.g. Tørseth et al. (2012), Lefohn et al. (2018). These trends are actually observed for sites in Brussels (Paoletti et al., 2014) and for the Uccle site (see Fig. S8), although there seems to
455 be a levelling off in those opposite trends for low and high ozone concentrations since 2000 compared to the decade before. Finally, the trends in 11h30 UT surface ozone measurements can be impacted by changes in meteorology and weather regimes, or long-range transport patterns due to e.g. climate change.

To conclude, explaining the increasing mean surface ozone amounts in combination with the decreasing ozone precursor emissions at Uccle is less straightforward than the (opposing) trends in high and low level ozone concentrations. This is due
460 to the interplay of many factors such as meteorology, the non-linear dependence of the ozone concentrations on the emissions of VOC and NO_x , the dual role of NO_x as ozone source or sink depending on the season, and the amount of NO_x emissions.



465 **Figure 7:** Monthly mean time series of Uccle surface ozone (upper panel, black) and mean ozone in the lowest 1 km above Uccle from the ozonesonde launches (upper panel, green) and ozone precursor measurements at Uccle (NO, NO₂) and Elsene (CO, 5 km from Uccle). Linear trends are shown, together with the absolute and relative trend estimates (calculated from monthly anomalies), and their 2 σ uncertainties. The monthly anomaly time series of these measurements can be found in Fig. S7.

5 Validation of satellite ozone retrievals with Uccle ozonesonde data

470 Ozonesondes are virtually all-weather, i.e., unaffected by clouds and precipitation, in contrast to most spectroscopic techniques, and they provide high vertical resolution ozone profiles from the ground to about 30 km. Therefore, satellite algorithms are based on ozonesonde climatologies and in turn satellites are validated by the sondes. Since the start of the ozone measuring satellite era, ozone profiles from soundings at Uccle have been used for validation of satellite ozone retrievals, e.g. the Stratospheric Aerosol and Gas Experiment (SAGE) II satellite profiles (Attmannspacher et al., 1989, De Muer et al., 1990). In this section, we give some recent examples of the application of the Uccle ozone profile data for operational satellite validation (Sect. 5.1), and for the scientific evaluation of both stratospheric (Sect. 5.2) and tropospheric (Sect. 5.3) ozone profile retrievals by satellite instruments. In these latter two sections, we also illustrate that a consistent and homogenous ozonesonde dataset like the Uccle one is crucial to determine the long-term stability of (merged) satellite ozone retrievals.



480 5.1 Operational validation within EUMETSAT AC-SAF

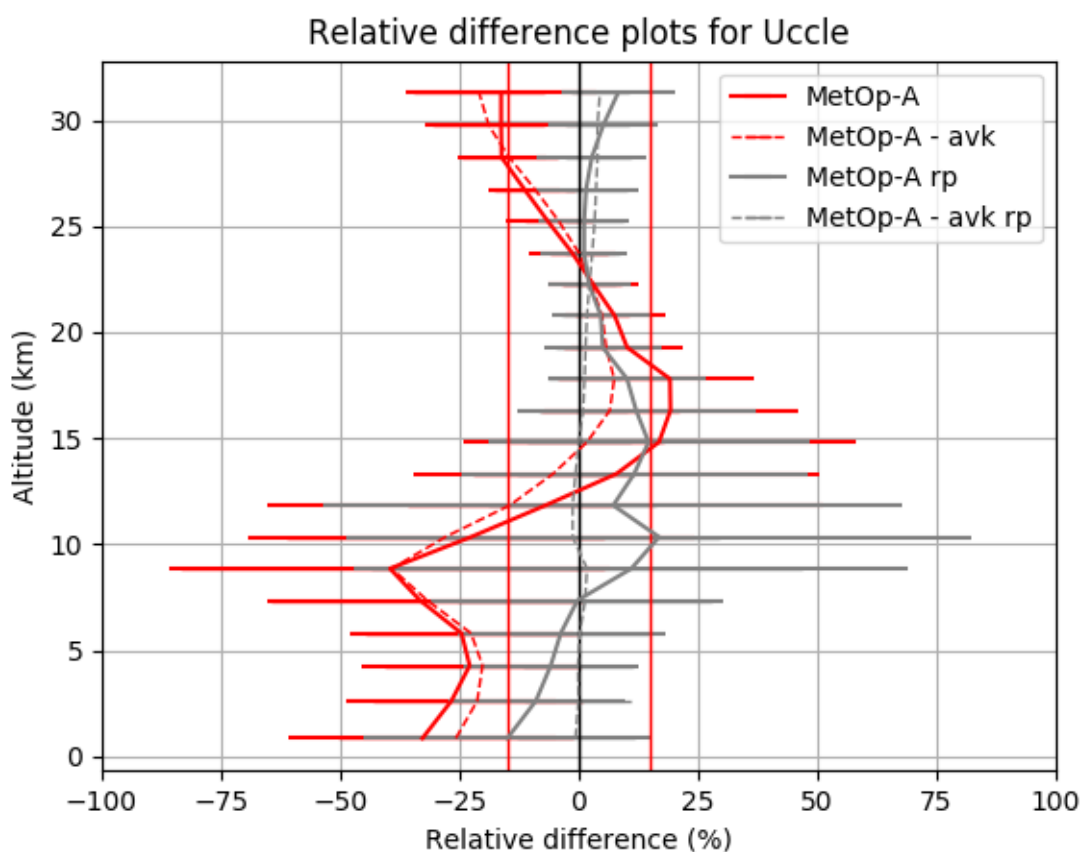
As partner of the EUMETSAT Atmospheric Composition Satellite Application Facilities (AC SAF), RMI is responsible for the validation of different ozone (ozone profiles and (tropical) tropospheric ozone columns) and aerosol products (Hassinen et al., 2016, Valks et al., 2014, van Peet et al., 2014) from GOME-2 and Infrared Atmospheric Sounder Interferometer (IASI) instruments on board the MetOp A/B/C satellite platforms. Those different instruments give us the opportunity to
485 obtain a unique dataset, retrieved with an identical technique, from the beginning of the MetOp-A/GOME-2 instrument in 2007, until the end of the third, MetOp-C/GOME-2, foreseen in 2022. GOME-2 ozone profiles are given as partial ozone columns, expressed in Dobson Units, on 40 varying pressure levels between the surface level and 0.001 hPa and are calculated by the Ozone Profile Retrieval Algorithm (OPERA, van Peet et al., 2014). The a-priori information used for the retrieval is obtained from McPeters and Labow (2012).

490 For the validation of GOME-2 ozone profiles within the AC-SAF, ozonesonde measurements are extensively used. However, for a meaningful comparison, the ozonesonde profiles need to be integrated first between the GOME-2 pressure levels. When comparing a single ozonesonde profile with different GOME-2 profiles, the actual reference ozone values are not identical due to the fact that the GOME-2 vertical levels vary from one measurement to another. GOME-2 has a nominal spatial resolution of 80 km x 40 km, but for the shortest UV wavelengths the integration time takes eight times longer
495 because of the lower number of photons arriving on the detector pixels. Secondly, as the ozonesondes and the satellite do not have the same vertical resolution, it is necessary to take into account the averaging kernels (AVK), to “smooth” the ozone soundings towards the resolution of the satellite (Rodgers, 2000).

In Figure 8 the relative differences between the MetOp-A operational ozone profile product and the Uccle ozonesonde profiles are shown for the year 2018 (red colour). The following co-location criteria were applied: a geographic distance of
500 less than 100 km between the GOME-2 pixel centre and the sounding station location, and a time difference of less than 10 hours between the pixel sensing and the sounding launch time. The figure highlights two different aspects of the operational validation. First, it can be noted that applying the averaging kernels to the sounding profiles improves the comparison with the GOME-2 ozone product significantly, i.e. by 15%, in particular in the lower stratosphere (compare the full lines with dashed lines in Fig. 8). Moreover, as the GOME-2 ozone profile product is based on UV measurements, it is sensitive to
505 degradation of the UV sensor (van Peet et al., 2014, Munro et al., 2016). Therefore, a degradation correction has been developed for the MetOp-A data, already launched in 2007, and applied to the data for the relative differences with the Uccle data in Fig. 8 (in grey). From this figure, it should be clear that this degradation correction improves significantly the agreement with the Uccle ozonesonde data compared to the operational product (in red), resulting in relative differences between GOME-2 ozone profiles and the Uccle data within the target error range of 15% (marked by the vertical red lines).
510 The improvement after degradation correction is a promising result, showing the challenge for UV-VIS sounders to obtain a stable ozone profile product on different sensors (GOME-2A/2B/2C) for different periods using the same type of optical



instrument. More feedback on the status of this operational EUMETSAT product can be obtained in the validation reports, available on the AC SAF website (<https://acsaf.org>, e.g. Delcloo and Kreher, 2013).



515

Figure 8: Relative mean differences and standard deviations between ozone profiles retrieved from MetOp-A/GOME-2 and Uccle ozone profiles for the time period January to December 2018. The red graph represents the mean differences when using the operational MetOp-A/GOME-2 product, the grey graph when the UV sensor degradation correction has been applied in the MetOp-A/GOME-2 ozone retrieval. Relative mean differences denoted by dashed lines are obtained after applying the averaging kernel to the Uccle sounding data. Finally, the thin red vertical lines mark the $\pm 15\%$ target error range of the MetOp-A/GOME-2 ozone profile product.

520

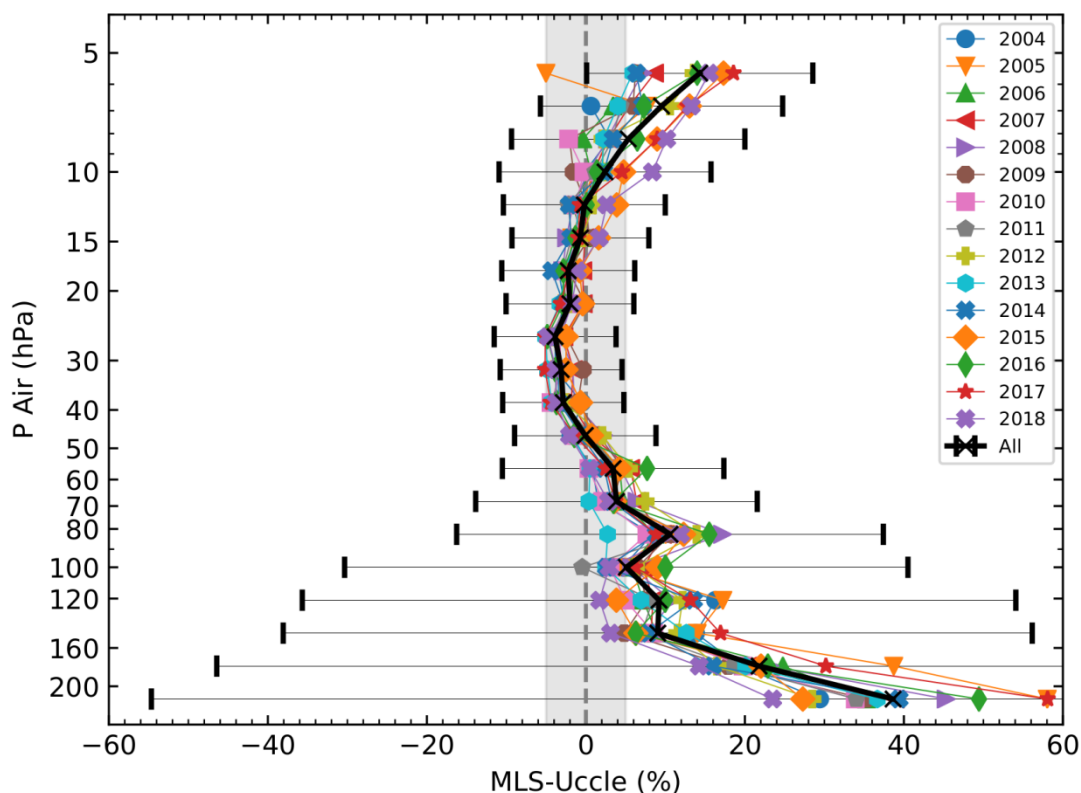
5.2 Validation of AURA-MLS stratospheric ozone profiles

The Microwave Limb Sounder (MLS, Froidevaux et al., 2008) is one of the four instruments on the Earth Observing System (EOS) Aura Satellite. MLS has been measuring vertical profiles of atmospheric trace gases, including ozone, along with temperature, geopotential height, relative humidity, cloud ice water content and cloud ice water path, since its launch in 2004. Global measurements (from 82° S to 82° N) at two fixed solar times, noon-night, at around 01:30 a.m./p.m. are achieved, with the number of profiles over e.g. ozonesonde sites varying between 0 and 6 daily. MLS products have been

525



validated to be very accurate and stable (Jiang et al., 2007, Froidevaux et al., 2008), and have been used in many studies involving ozonesonde measurements (e.g. Witte et al., 2017, Stauffer et al., 2020). Here, we have implemented the latest
530 MLS v4.2 data, screened according to the v4.2 Level 2 MLS Data Quality document (Livesey et al., 2020) and compared the satellite overpass measurements, without averaging kernel, with coincident ozonesonde profiles at Uccle. Because there are multiple profiles crossing over Uccle at a fixed time, the profile closest in distance is used for the validation. Both the noon and night overpasses have been used, as we did not find significant differences between those. As a result, ~3000 profiles were included into the validation. To account for the difference in resolution, Uccle ozonesonde data are linearly interpolated
535 to the MLS vertical resolution (between 3-6 km, depending on the altitude). The mean annual relative differences between MLS and Uccle ozonesondes are shown in Fig. 9. Different conclusions can be drawn from this figure. First, MLS and the Uccle ozonesondes compare very well, within $\pm 5\%$ between 10 and 70 hPa (grey shading in Fig. 9). At pressures smaller than 10 hPa, ozonesonde measurements are known to be less accurate (see also Sect. 2.2), while at pressures larger than 70 hPa, the MLS ozone retrieval is more challenging because of the longer atmospheric path and the lower ozone volume
540 mixing ratios increasing the relative differences. Another important finding from this figure is that the mean annual relative differences are very consistent over the different years, which means that both the MLS instrument and the Uccle ozonesonde time series are very stable with respect to each other. In addition to this (see Fig. S9), we also want to mention that the relative differences between MLS and Uccle ozonesondes are very similar for the different seasons.



545 **Figure 9: Relative ozone profile differences between MLS and Uccle ozonesonde. The different colours correspond to the different**
550 **years and the black line to the overall relative difference. The error bar is only shown for the overall and corresponds to one**
standard deviation.

5.3 Validation of AURA-TES tropospheric ozone profiles

Here we compare the tropospheric vertical ozone profiles of the Uccle sondes coinciding with the observations from the
550 Tropospheric Emission Spectrometer (TES) sensor on-board the Aura satellite for the period late 2004 to early 2018. TES is
an infrared Fourier transform spectrometer (Beer et al., 2001; Beer, 2006) following a near-polar, sun-synchronous orbit with
equator crossing times of 13:40 local mean solar time for the ascending part of the orbit. TES is predominantly nadir viewing
and measures radiance spectra of Earth's atmosphere at wavelengths between 3.3 and 15.4 μm . The nadir vertical profiles are
spaced 1.6° apart along the orbit track and have a footprint of approximately $5 \times 8 \text{ km}^2$ (Beer et al., 2001; Beer, 2006).
555 The vertical sensitivity of the TES-retrieved ozone is the largest for the troposphere, with a vertical resolution for ozone
profiles of 6-7 km, corresponding to 1-2 degrees of freedom in the troposphere (Jourdain et al., 2007). Prior to applying TES
ozone data, they are subject to screening using the TES ozone master quality flag that accounts for clouds and too large
difference between observed and simulated radiances (Osterman et al., 2008).



As in Nasser et al. (2008), we apply temporal and spatial coincidence criteria of ± 9 h and ± 300 km respectively between the
560 sonde and TES observations. These criteria can provide enough profiles for a statistically meaningful comparison while it is
sufficiently strict to warrant a high probability that both instruments sample similar air masses. A mapping matrix is used to
interpolate the sonde data to the 67-level pressure grid (from 1212 to 0.1 hPa) used in the TES retrievals. Then, the TES
observation operator was applied to the 67-level pressure grid of the Uccle sonde data to ensure a consistent comparison
between TES and ozonesonde data excluding the influence of the a priori ozone profile needed to regulate the TES retrieval
565 (Verstraeten et al., 2013).

By applying all these constraints (coinciding criteria and the TES ozone master flag) 191 suitable coincidences or data pairs
for the full time range from 2004 to 2018 were collected. Figure 10 presents TES–sonde tropospheric ozone profile
differences for the Uccle sondes. The left panel shows the absolute ozone vertical profile differences (TES–sonde) in the
troposphere (1000–300 hPa). The right panel shows the relative differences ($(\text{TES} - \text{sonde}) \times 100 / \text{sonde}$) for the full vertical
570 ozone profile (1000–1 hPa).

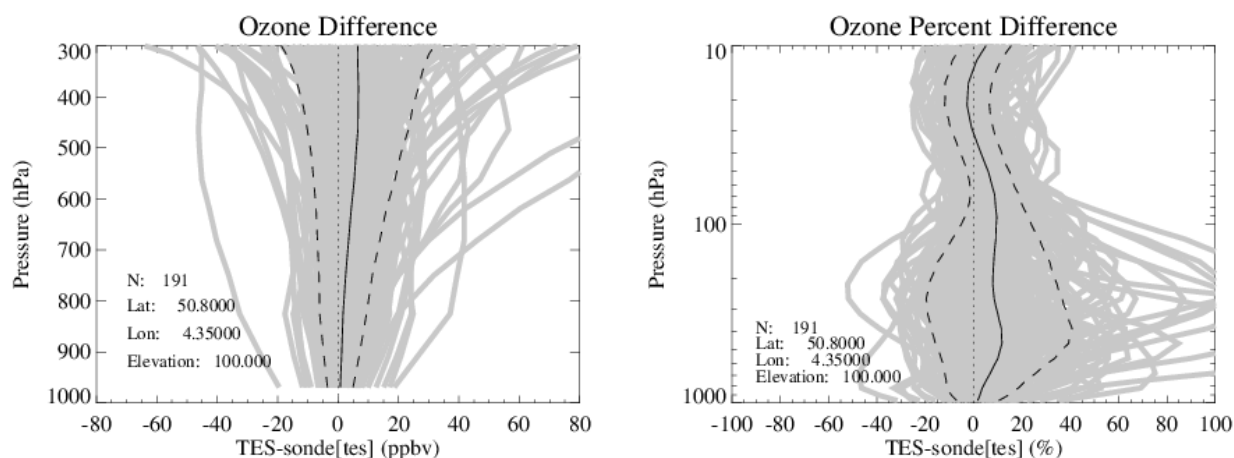


Figure 10: Absolute TES–sonde tropospheric ozone vertical differences (left) and relative differences (right) for the whole profile of Uccle. Individual difference profiles are shown in grey; the mean difference and one standard deviation profiles are in black. N is the number of valid profiles after flagging TES data and using the maximum 300 km and 9h coinciding criteria.

575 Figure 10 indicates that TES is generally positively biased within the troposphere by up to ~ 10 ppbv, corresponding to
relative differences up to ~ 15 %. The TES bias slightly varies as a function of pressure. TES appears to be almost unbiased
with respect to the sondes in the lower troposphere, but this actually reflects the non-sensitivity of TES to ozone in the lower
atmosphere for situations with lower brightness temperature as encountered at higher latitudes. Since the TES signal in the
troposphere has typically 1–2 degrees of freedom, analysing the TES bias for two vertical regimes - the lower troposphere
580 (LT, 1000 to 500 hPa) and the upper troposphere (UT, 500 hPa to tropopause)- might be meaningful (Nassar et al., 2008).
From a linear regression of all TES vs. sonde ozone data pairs for Uccle in the lower troposphere, we find a slope of 0.90
with an intercept of 7.98 ($R = 0.60$) with a bias of +2.96 ppbv. For the upper troposphere the bias is a bit higher (7.80 ppbv),



the correlation (R) is 0.89 and the slope and intercept are 0.99 and 8.75 respectively. These values are in line with reported ones for data pairs collected for the whole northern mid-latitudes (Verstraeten et al., 2013).

585 The temporal stability of the TES sensor for tropospheric ozone can be assessed by applying the Theil Sen trend statistics (Theil 1950a, 1950b, 1950c; Sen, 1968) on the time series of the TES-sonde data pairs for each pressure level in the troposphere (surface to 300 hPa). Analysis shows that all p -values are larger than 0.05 indicating that all slopes of the linear regression are not statistically different from zero in the troposphere. All R^2 values are smaller than 0.01. Thus, there is no reason to assume any temporal trend for data pairs in the troposphere. This is in line with the same analysis for the 464 hPa

590 level by Verstraeten et al. (2013).

6 Conclusions and outlook

Having started operationally in 1969 to use ozone as a tracer to study the general air circulation in the troposphere and the lower stratosphere, the high-frequency (three times/week) mid-latitude Uccle ozone sounding time series now extends over more than 50 years, covering around 7000 profiles. Over this entire period, attention has always been paid to the consistency

595 of the time series, resulting in only one major change: the switch from BM to En-Sci ECC sondes in 1997. This change was however well documented with dual launches and pump efficiency laboratory measurements of both pump types, so that a unique correction method for both sonde types, a PRESSure and Temperature dependent total Ozone normalization (PRESTO, Van Malderen et al., 2016), has been developed (De Backer et al., 1998a,b) to guarantee the data homogeneity. Another distinct feature of the Uccle ozonesonde dataset is the correction for urban SO_2 interference with the chemical

600 reactions in the ozone cells in the first half of the period.

Although satellites provide global routine measurements of ozone profiles with increasing accuracy and spatial resolution, ozonesondes are the only technique that can provide, since 50 years, accurate (around 5-10%), vertically resolved observations from the surface up to the lower stratosphere, unaffected by clouds or precipitation. Furthermore, they can resolve strong gradients in the UTLS (upper troposphere/lower stratosphere), while precisely locating the thermal tropopause

605 (Thompson et al., 2011). In this paper, we illustrated the importance of the Uccle ozonesonde dataset in two specific application areas: for the assessment of the long-term vertical ozone trends and for the validation of satellite retrievals of ozone profiles. The strength of the ozonesonde measurements (and the Uccle time series in particular) lies exactly in combining those two aspects of ozone research, together with its applicability in process studies. The major conclusions are summarized here.

610 Making use of the LOTUS multiple linear regression model including the QBO, the solar radio flux, ENSO, and AOD as explanatory variables, we found that the stratospheric ozone concentrations at Uccle declined at a significant rate of around 2%/decade since 1969. This overall decline can mainly be attributed to the increasing ODS emissions, with a rather consistent decline rate around -4%/decade for the period 1969-1996. Since 2000, a recovery between +1-3%/decade of the stratospheric ozone levels above Uccle is observed, although not significant and not for the upper stratospheric levels



615 measured by ozonesondes. A significant decline in lower stratospheric ozone amounts since 1998, as reported by Ball et al.
(2018, 2019), is hence not present in the Uccle and nearby De Bilt time series. For the considered periods, we found an
overall agreement between the sign of the stratospheric temperature trends and those ozone concentration trends, i.e. a
cooling of the stratosphere in 1969-2018 and 1969-1996 and an insignificant warming for all but the lower stratospheric
layers since 2000, underlining the possible mutual interaction between stratospheric ozone concentration and temperature
620 changes.

The total ozone loss between 1971-1996 (at a rate of $-2.5\%/decade$) is almost entirely compensated by the gain
($+2\%/decade$) between 1997-2019. In the light of the discussion on the stratospheric ozone trends in the previous paragraph,
this would mean that the tropospheric ozone amounts at Uccle should increase since the mid-90s. We indeed confirmed a
very consistent increase of the ozone concentrations at 2 to 3 $\%/decade$ throughout the entire free troposphere, a number
625 which is in almost perfect agreement with the trends derived from the IAGOS ascent/descent profiles at Frankfurt, and
1 $\%/decade$ lower than the De Bilt tropospheric ozone trends. The Uccle 1995-2019 trend is even 0.5 to 1 $\%/decade$ higher
than the 1969-2019 trend. Despite the levelling off in tropospheric ozone precursor emissions, the tropospheric ozone
amounts in Uccle are still increasing. Based on chemistry-climate model calculations, Griffiths et al. (2020) found that an
increase in the tropospheric ozone burden might be driven by increased stratosphere-to-troposphere transport of recovering
630 stratospheric ozone. It should also be noted that the amount of tropopause folding events in the Uccle time series increased
significantly over time, which might be an indicator for increased transport of ozone from the stratosphere into the
troposphere. However, also the surface ozone trends behave similarly: the concentrations of precursor trace gases CO, NO,
and NO₂ have significantly decreased, but the surface ozone concentrations continue to increase since the beginning of those
measurements in the 1980s and 1990s. To explain this, we should keep in mind that Uccle is a (sub)urban site, and in such an
635 environment of elevated NO_x concentrations, the photochemical production of ozone might lead to rising concentrations,
even with declining NO_x emissions.

For the operational validation of the GOME-2 and IASI ozone profiles within the EUMETSAT AC-SAF, the role of
ozonesonde profiles is crucial. We showed how the Uccle dataset can be used to evaluate the performance of a degradation
correction for the GOME-2 UV sensors. The Uccle ozonesondes are also used to assess the accuracy and stability of satellite
640 ozone retrievals. Here, we showed that the AURA-MLS overpass ozone profiles agree very well with the ozonesonde
profiles, within $\pm 5\%$ between 10 and 70 hPa. Another instrument on the same AURA satellite platform, TES, has its largest
vertical sensitivity for ozone in the troposphere, and is generally positively biased with respect to the Uccle ozonesondes in
the troposphere by up to ~ 10 ppbv, corresponding to relative differences up to $\sim 15\%$. Using the Uccle ozonesonde data
series as reference, we also found that the temporal stability of both satellite retrievals is excellent. Vice versa, satellite total
645 ozone retrievals and MLS have enabled the detection of a post-2013 drop-off in total ozone at a third of global ozonesonde
stations (Stauffer et al., 2020). Our analysis with MLS here confirmed their finding that Uccle is not affected by any total
column drop-off of more than 3% in its time series.



A higher flexibility of ozonesonde launch times toward satellite overpass times is an emerging issue that needs to be considered against the preference for a fixed launch time for e.g. the assessment of tropospheric ozone trends. Moreover, for over a decade, weather prediction centres have been incorporating chemistry into operational forecasts, assimilating satellite ozone retrievals, and ozonesondes are used for external evaluation of those model forecasts (e.g. for tropospheric ozone: Flemming et al., 2015), analyses (e.g. for stratospheric ozone: Lefever et al., 2015) and reanalyses (e.g. Inness et al, 2019). Those services require a near real-time delivery of the ozonesonde measurements, with an operational quality assessment/quality control tool, as the total column ozone drop-off in a third of the ozonesonde stations (Stauffer et al., 2020) made obvious. These are the challenges for operational applications of ozonesondes. For the assessment of the long-term variability of ozone concentrations at different atmospheric altitudes and the interaction between climate change and ozone (also studied in coupled chemistry-climate and chemistry-transport models, see e.g. Morgenstern et al., 2017), the availability of a long-term homogeneous dataset is crucial. Homogenization efforts of ozonesonde networks and/or datasets (Tarasick et al., 2016; Van Malderen et al., 2016; Thompson et al., 2017; Witte et al., 2017, 2018, 2019; Sterling et al., 2018) should therefore be continued and extended. With these developments in mind, we aim at continuing the pioneering role that the Uccle time series had in some of the research areas during its half a century lifetime.

Code/Data availability

The ozonesonde and total column ozone data used in this paper is publicly available through the World Ozone and Ultraviolet Radiation Data Centre (WOUDC) and the Network for the Detection of Atmospheric Composition Change (NDACC). The MOZAIC/CARIBIC/IAGOS data are available at <http://www.iagos.fr> and the surface ozone and ozone precursor data at Uccle can be found at <http://www.irceline.be>, the website of IRCEL-CELINE (Belgian Interregional Environment Agency). The AURA MLS v4.2 Uccle overpass data were obtained at <http://avdc.gsfc.nasa.gov/pub>, the TES data at <https://search.earthdata.nasa.gov/>. The source code of the LOTUS regression model is publicly available at https://arg.usask.ca/docs/LOTUS_regression.

Author Contribution

RVM prepared the manuscript, with contributions from all authors. DDM wrote and took the lead of Sect. 2, HDB wrote Sect. 2.2.3 and made Fig. 3 in Sect. 4.1. DDM and HDB developed the ozonesonde data processing method and tools. DP performed the analysis for Sect. 4.2 and 5.2, and wrote Sect. 5.2. WWV wrote and did the analysis for Sect. 5.3 and helped in preparing Sect. 4.3. VDB performed part of the analysis in Sect. 4.3 and wrote that part. AD wrote and did the analysis for Sect. 5.1. MA provided the De Bilt ozonesonde dataset and gave feedback. FF provided the surface ozone and ozone



precursor data at Uccle, prepared Fig. S8, and helped in preparing Sect. 4.3 and 4.4. VT gave guidance on the use of the IAGOS data at Frankfurt airport. All authors provided comments on the manuscript.

Competing Interests

680 The authors declare that they have no conflict of interest.

Acknowledgements

The Uccle ozone sounding time series could only be built up thanks to the efforts and dedication of the ozone sounding operators over the past 50 years (Martin Lebrun, Jean-Claude Grymonpont, André Massy, Jozef Bartholomees, Daniel Watez, Eli Weerts, Kevin Knockaert, and Roger Ameloot) and the technical support by Geert Desadelaer. Since 2007, the
685 ozone sounding program in Uccle and R. Van Malderen are funded by the Solar-Terrestrial Centre of Excellence (STCE), a research collaboration established by the Belgian Federal Government through the action plan for reinforcement of the federal scientific institutes. We are grateful to WOUDC and the NDACC for archiving the (Uccle) ozone data and making them publicly available. The MOZAIC/CARIBIC/IAGOS data were created with support from the European Commission, national agencies in Germany (BMBF), France (MESR), and the UK (NERC), and the IAGOS member institutions
690 (<http://www.iagos.org/partners>). The participating airlines (Lufthansa, Air France, Austrian, China Airlines, Iberia, Cathay Pacific, Air Namibia, and Sabena) supported IAGOS by carrying the measurement equipment free of charge since 1994. The data are available at <http://www.iagos.fr> thanks to additional support from AERIS. We would like to thank our colleagues from the panel for Assessment of Standard Operating Procedures for Ozonesondes (ASOPOS) for many constructive discussions about the functioning and exploitation of ozonesonde data, and in particular Herman Smit, chair of this panel.
695 We are indebted to Daniel Zawada at the University of Saskatchewan, Canada, for his help with implementing the LOTUS regression model. We also thank Daan Hubert from the Royal Belgian Institute for Space Aeronomy for some comments on an earlier version of the manuscript.

References

- 700 Antonescu, B., Vaughan, G., and Schultz, D. M.: A Five-Year Radar-Based Climatology of Tropopause Folds and Deep Convection over Wales, United Kingdom, *Mon. Wea. Rev.*, 141, 1693–1707, <https://doi.org/10.1175/MWR-D-12-00246.1>, 2013.
- Aquila, V., Oman, L. D., Stolarski, R., Douglass, A. R., and Newman, P. A.: The Response of Ozone and Nitrogen Dioxide to the Eruption of Mt. Pinatubo at Southern and Northern Midlatitudes. *J. Atmos. Sci.*, 70, 894–900, <https://doi.org/10.1175/JAS-D-12-0143.1>, 2013.



- 705 Attmannspacher, W., and Dütsch, H. U.: International ozonesonde intercomparison at the Observatory Hohenpeissenberg 19 January - 5 February 1970, *Berichte des Deutschen Wetterdienstes Nr. 120*, Offenbach a. M., 1970.
- Attmannspacher, W., and Dütsch H. U.: 2nd International ozonesonde intercomparison at the Observatory Hohenpeissenberg 5 - 20 April 1978, *Berichte des Deutschen Wetterdienstes Nr. 157*, Offenbach a. M., 1981.
- Attmannspacher, W., de la Noé, J., de Muer, D., Lenoble, J., Mégie, G., Pelon, J., Pruvost, P., and Reiter, R.: European
710 validation of SAGE II ozone profiles, *J. Geophys. Res.*, 94 (D6), 8461– 8466, doi:10.1029/JD094iD06p08461, 1989.
- Ball, W. T., Alsing, J., Mortlock, D. J., Staehelin, J., Haigh, J. D., Peter, T., Tummon, F., Stübi, R., Stenke, A., Anderson, J., Bourassa, A., Davis, S. M., Degenstein, D., Frith, S., Froidevaux, L., Roth, C., Sofieva, V., Wang, R., Wild, J., Yu, P., Ziemke, J. R., and Rozanov, E. V.: Evidence for a continuous decline in lower stratospheric ozone offsetting ozone layer recovery, *Atmos. Chem. Phys.*, 18, 1379–1394, <https://doi.org/10.5194/acp-18-1379-2018>, 2018.
- 715 Ball, W. T., Alsing, J., Staehelin, J., Davis, S. M., Froidevaux, L., and Peter, T.: Stratospheric ozone trends for 1985–2018: sensitivity to recent large variability, *Atmos. Chem. Phys.*, 19, 12731–12748, <https://doi.org/10.5194/acp-19-12731-2019>, 2019
- Beekmann, M., Ancellet, G., Blonsky, S., De Muer, D., Ebel, A., Elbern, H., Hendricks, J., Kowol, J., Mancier, C., Sladkovic, R., Smit, H. G. J., Speth, P., Trickl, T., Van Haver, Ph.: Regional and Global Tropopause Fold Occurrence and
720 Related Ozone Flux Across the Tropopause, *J. Atmos. Chem.*, 28, 29–44, <https://doi.org/10.1023/A:1005897314623>, 1997.
- Beer, R.: TES on the Aura Mission: Scientific Objectives, Measurements and Analysis Overview, *IEEE T. Geosci. Remote Sens.*, 44, 1102–1105, 2006.
- Beer, R., Glavich, T. A., and Rider, D. M.: Tropospheric Emission Spectrometer for the Earth Observing System's Aura satellite, *Appl. Optics*, 40, 2356–2367, 2001.
- 725 Brewer, A. W., and Milford, J.R.:The Oxford-Kew ozone sonde, *Proc. R. Soc. London, Ser. A*, 256, 470– 495, 1960.
- Butchart, N.: The Brewer-Dobson circulation, *Rev. Geophys.*, 52, 157–184, doi:10.1002/2013RG000448, 2014.
- Chang, K-L, Petropavlovskikh, I, Cooper, O. R., Schultz, M. G., and Wang, T.: Regional trend analysis of surface ozone observations from monitoring networks in eastern North America, Europe and East Asia., *Elem Sci Anth*, 5, p.50. doi: <http://doi.org/10.1525/elementa.243>, 2017.
- 730 Chang, K.-L., Cooper, O. R., Gaudel, A., Petropavlovskikh, I., and Thouret, V.: Statistical regularization for trend detection: an integrated approach for detecting long-term trends from sparse tropospheric ozone profiles, *Atmos. Chem. Phys.*, 20, 9915–9938, <https://doi.org/10.5194/acp-20-9915-2020>, 2020.
- Chipperfield, M. P., Dhomse, S., Hossaini, R., Feng, W., Santee, M. L., Weber, M., Burrows, J. P., Wild, J. D., Loyola, D., Coldewey-Egbers, M.: On the cause of recent variations in lower stratospheric ozone, *Geophys. Res. Lett.*, 45, 5718–5726.
735 <https://doi.org/10.1029/2018GL078071>, 2018.
- Cooper, O. R., Parrish, D. D., Ziemke, J., Balashov, N. V., Cupeiro, M., Galbally, I. E., Gilge, S., Horowitz, L., Jensen, N. R., Lamarque, J.-F., Naik, V., Oltmans, S. J., Schwab, J., Shindell, D. T., Thompson, A. M., Thouret, V., Wang, Y. and



- Zbinden, R. M.: Global distribution and trends of tropospheric ozone: An observation-based review, *Elem Sci Anth*, 2, p.000029, doi: <http://doi.org/10.12952/journal.elementa.000029>, 2014.
- 740 Cooper, O. R., Schultz, M. G., Schroeder, S., Chang, K.-L., Gaudel, A., Benítez, G. C., Cuevas, E., Fröhlich, M., Galbally, I. E., Molloy, S., Kubistin, D., Lu, X., McClure-Begley, A., Nédélec, P., O'Brien, J., Oltmans, S. J., Petropavlovskikh, I., Ries, L., Senik, I., Sjöberg, K., Solberg, S., Spain, G.T., Spangl, W., Steinbacher, M., Tarasick, D., Thouret, V. and Xu, X.: Multi-decadal surface ozone trends at globally distributed remote locations, *Elem Sci Anth*, 8(1), p.23. doi: <http://doi.org/10.1525/elementa.420>, 2020.
- 745 De Backer H. and De Muer, D.: Intercomparison of total ozone data with Dobson and Brewer ozone spectrophotometers at Uccle (Belgium) from January 1984 to March 1991, including zenith sky observations, *J. Geophys. Res.*, 96, 20711-20719, 1991.
- De Backer, H.: Analysis and interpretation of ozone observations at Uccle (1969-1993), Ph. D. thesis, Vrije Universiteit Brussel, 160pp, 1994.
- 750 De Backer, H., De Muer, D., Schoubs, E. and Allaart, M.: A new pump correction profile for Brewer-Mast ozonesondes, in *Proceedings of the 18th Quadrennial Ozone Symposium*, edited by R. Bojkov and G. Visconti, Parco Scientifico e Tecnologico d'Abruzzo, Italy, 891-894, 1998a.
- De Backer H., De Muer, D., and De Sadelaer, G.: Comparison of ozone profiles obtained with Brewer-Mast and Z-ECC sensors during simultaneous ascents, *J. Geophys. Res.* 103, 19641-19648, 1998b.
- 755 De Backer, H.: Homogenisation of ozone vertical profile measurements at Uccle, *Wetenschappelijke en technische publicaties van het K.M.I. no 7*, ISSN D1999/0224/007, K.M.I., 26pp, Ukkel, 1999.
- Delcloo, A. and Kreher K.: Validation report on GOME-2 near real-time and offline high-resolution ozone profiles, available at https://acsaf.org/docs/vr/Validation_Report_NOP_NHP_OOP_OHP_Jun_2013.pdf, 2013.
- De Muer, D.: A correction procedure for electrochemical ozone soundings and its implication for the tropospheric ozone budget, *Proc. of the Quadrennial International Ozone Symposium*, Boulder, Colorado 4-9 Aug. 1980, Vol. I, 88-95, 1981.
- 760 De Muer D., De Backer, H., Veiga, R., and Zawodny, J.: Comparison of SAGE II ozone measurements and ozone soundings at Uccle (Belgium) during the period February 1985 to January 1986, *J. Geophys. Res.*, 95, 11903-11911, 1990.
- De Muer D. and De Backer, H.: Revision of 20 years of Dobson total ozone data at Uccle (Belgium): Fictitious Dobson total ozone trends induced by sulfur dioxide trends, *J. Geophys. Res.*, 97, 5921-5937, 1992.
- 765 De Muer D. and De Backer, H.: Influence of sulfur dioxide trends on Dobson measurements and on electrochemical ozone soundings, *SPIE*, 2047, 18-26, 1993.
- De Muer D. and De Backer, H.: The discrepancy between stratospheric ozone profiles from balloon soundings and from other techniques: a possible explanation, *Proc. of the Quadrennial Ozone Symposium*, Charlottesville, USA, June 4-13 1992, 815-818, 1994.
- 770 De Muer D. and Malcorps, H.: The frequency response of an electrochemical ozone sonde and its application to the deconvolution of ozone profiles, *J. Geophys. Res.* 89, 1361-1372, 1984.



- Flemming, J., Huijnen, V., Arteta, J., Bechtold, P., Beljaars, A., Blechschmidt, A.-M., Diamantakis, M., Engelen, R. J., Gaudel, A., Inness, A., Jones, L., Josse, B., Katragkou, E., Marecal, V., Peuch, V.-H., Richter, A., Schultz, M. G., Stein, O., and Tsikerdekis, A.: Tropospheric chemistry in the Integrated Forecasting System of ECMWF, *Geosci. Model Dev.*, 8, 975–1003, <https://doi.org/10.5194/gmd-8-975-2015>, 2015.
- 775 Froidevaux, L., Jiang, Y. B., Lambert, A., Livesey, N. J., Read, W. G., Waters, J. W., Browell, E. V., Hair J. W., Avery M. A., McGee T. J., Twigg, L. W., Sumnicht, G. K., Jucks, K. W., Margitan, J. J., Sen, B., Stachnik R. A., Toon G. C., Bernath, P. F., Boone, C. D., Walker, K. A., Filipiak, M. J., Harwood, R. S., Fuller, R. A., Manney, G. L., Schwartz, M. J., Daffer, W. H., Drouin, B. J., Cofield, R. E., Cuddy, D. T., Jarnot, R. F., Knosp, B. W., Perun, V. S., Snyder, W. V., Stek, P. C., 780 Thurstans, R. P., and Wagner, P. A.: Validation of Aura Microwave Limb Sounder stratospheric ozone measurements, *J. Geophys. Res.*, 113, D15S20, doi:10.1029/2007JD008771, 2008.
- Gaudel, A., Cooper, O.R., Ancellet, G., Barret, B., Boynard, A., Burrows, J.P., Clerbaux, C., Coheur, P.-F., Cuesta, J., Cuevas, E., Doniki, S., Dufour, G., Ebojje, F., Foret, G., Garcia, O., Granados Muñoz, M.J., Hannigan, J.W., Hase, F., Huang, G., Hassler, B., Hurtmans, D., Jaffe, D., Jones, N., Kalabokas, P., Kerridge, B., Kulawik, S.S., Latter, B., Leblanc, 785 T., Le Flochmoën, E., Lin, W., Liu, J., Liu, X., Mahieu, E., McClure-Begley, A., Neu, J.L., Osman, M., Palm, M., Petetin, H., Petropavlovskikh, I., Querel, R., Rahpoe, N., Rozanov, A., Schultz, M.G., Schwab, J., Siddans, R., Smale, D., Steinbacher, M., Tanimoto, H., Tarasick, D.W., Thouret, V., Thompson, A.M., Trickl, T., Weatherhead, E., Wespes, C., Worden, H.M., Vigouroux, C., Xu, X., Zeng, G. and Ziemke, J., 2018. Tropospheric Ozone Assessment Report: Present-day distribution and trends of tropospheric ozone relevant to climate and global atmospheric chemistry model evaluation, *Elem Sci Anth*, 6(1), p.39. doi: <http://doi.org/10.1525/elementa.291>
- 790 Griffiths, P. T., Keeble, J., Shin, Y. M., Abraham, N. L., Archibald, A. T., and Pyle, J. A.: On the changing role of the stratosphere on the tropospheric ozone budget: 1979–2010, *Geophys. Res. Lett.*, 47, e2019GL086901, <https://doi.org/10.1029/2019GL086901>, 2020.
- Hassinen, S., Balis, D., Bauer, H., Begoin, M., Delcloo, A., Eleftheratos, K., Gimeno Garcia, S., Granville, J., Grossi, M., 795 Hao, N., Hedelt, P., Hendrick, F., Hess, M., Heue, K.-P., Hovila, J., Jönch-Sørensen, H., Kalakoski, N., Kauppi, A., Kiemle, S., Kins, L., Koukouli, M. E., Kujanpää, J., Lambert, J.-C., Lang, R., Lerot, C., Loyola, D., Pedergnana, M., Pinardi, G., Romahn, F., van Roozendaal, M., Lutz, R., De Smedt, I., Stammes, P., Steinbrecht, W., Tamminen, J., Theys, N., Tilstra, L. G., Tuinder, O. N. E., Valks, P., Zerefos, C., Zimmer, W., and Zyrichidou, I.: Overview of the O3M SAF GOME-2 operational atmospheric composition and UV radiation data products and data availability, *Atmos. Meas. Tech.*, 9, 383–407, 800 <https://doi.org/10.5194/amt-9-383-2016>, 2016.
- Hassler, B., Petropavlovskikh, I., Staehelin, J., August, T., Bhartia, P. K., Clerbaux, C., Degenstein, D., Mazière, M. D., Dinelli, B. M., Dudhia, A., Dufour, G., Frith, S. M., Froidevaux, L., Godin-Beekmann, S., Granville, J., Harris, N. R. P., Hoppel, K., Hubert, D., Kasai, Y., Kurylo, M. J., Kyrölä, E., Lambert, J.-C., Levelt, P. F., McElroy, C. T., McPeters, R. D., Munro, R., Nakajima, H., Parrish, A., Raspollini, P., Remsberg, E. E., Rosenlof, K. H., Rozanov, A., Sano, T., Sasano, Y., 805 Shiotani, M., Smit, H. G. J., Stiller, G., Tamminen, J., Tarasick, D. W., Urban, J., van der A, R. J., Veefkind, J. P.,



- Vigouroux, C., von Clarmann, T., von Savigny, C., Walker, K. A., Weber, M., Wild, J., and Zawodny, J. M.: Past changes in the vertical distribution of ozone – Part 1: Measurement techniques, uncertainties and availability, *Atmos. Meas. Tech.*, 7, 1395–1427, <https://doi.org/10.5194/amt-7-1395-2014>, 2014.
- Hering, W. S. and Dütsch, H.U.: Comparison of chemiluminescent and electrochemical ozonesonde observations, *J. Geophys. Res.*, 70, 5483-5490, 1965.
- 810 Hoesly, R. M., Smith, S. J., Feng, L., Klimont, Z., Janssens-Maenhout, G., Pitkanen, T., Seibert, J. J., Vu, L., Andres, R. J., Bolt, R. M., Bond, T. C., Dawidowski, L., Kholod, N., Kurokawa, J.-I., Li, M., Liu, L., Lu, Z., Moura, M. C. P., O'Rourke, P. R., and Zhang, Q.: Historical (1750–2014) anthropogenic emissions of reactive gases and aerosols from the Community Emissions Data System (CEDS), *Geosci. Model Dev.*, 11, 369–408, <https://doi.org/10.5194/gmd-11-369-2018>, 2018.
- 815 Inai, Y., Shiotani, M., Fujiwara, M., Hasebe, F., and Vömel, H.: Altitude misestimation caused by the Vaisala RS80 pressure bias and its impact on meteorological profiles, *Atmos. Meas. Tech.*, 8, 4043–4054, <https://doi.org/10.5194/amt-8-4043-2015>, 2015.
- Inness, A., Ades, M., Agustí-Panareda, A., Barré, J., Benedictow, A., Blechschmidt, A.-M., Dominguez, J. J., Engelen, R., Eskes, H., Flemming, J., Huijnen, V., Jones, L., Kipling, Z., Massart, S., Parrington, M., Peuch, V.-H., Razinger, M., Remy, S., Schulz, M., and Suttie, M.: The CAMS reanalysis of atmospheric composition, *Atmos. Chem. Phys.*, 19, 3515–3556, <https://doi.org/10.5194/acp-19-3515-2019>, 2019.
- 820 Jiang, Y. B., Froidevaux, L., Lambert, A., Livesey, N. J., Read, W. G., Waters, J. W., Bojkov, B., Leblanc, T., McDermid, I. S., Godin-Beekmann, S., Filipiak, M. J., Harwood, R. S., Fuller, R. A., Daffer, W. H., Drouin, B. J., Cofield, R. E., Cuddy, D. T., Jarnot, R. F., Knosp, B. W., Perun, V. S., Schwartz, M. J., Snyder, W. V., Stek, P. C., Thurstans, R. P., Wagner, P. A., Allaart, M., Andersen, S. B., Bodeker, G., Calpini, B., Claude, H., Coetzee, G., Davies, J., De Backer, H., Dier, H., Fujiwara, M., Johnson, B., Kelder, H., Leme, N. P., König-Langlo, G., Kyro, E., Laneve, G., Fook, L. S., Merrill, J., Morris, G., Newchurch, M., Oltmans, S., Parrondos, M. C., Posny, F., Schmidlin, F., Skrivankova, P., Stubi, R., Tarasick, D., Thompson, A., Thouret, V., Viatte, P., Vömel, H., von Der Gathen, P., Yela, M., and Zablocki, G.: Validation of Aura Microwave Limb Sounder Ozone by ozonesonde and lidar measurements, *J. Geophys. Res.*, 112, D24S34, <https://doi.org/10.1029/2007JD008776>, 2007.
- 830 Jourdain, L., Worden, H. M., Bowman, K., Li, Q. B., Eldering, A., Kulawik, S. S., Osterman, G., Boersma, K. F., Fisher, B., Rinsland, C. P., Beer, R., and Gunson, M.: Tropospheric vertical distribution of tropical Atlantic ozone observed by TES during the northern African biomass burning season, *Geophys. Res. Lett.*, 34, L04810, doi:10.1029/2006GL028284, 2007.
- Komhyr, W. D.: Electrochemical concentration cells for gas analysis, *Ann. Geophys.*, 25(1), 203–210, 1969.
- 835 Komhyr, W. D. and Evans, R. D.: Dobson spectrophotometer total ozone measurement errors caused by interfering absorbing species such as SO₂, NO₂ and photochemically produced O₃ in polluted air, *Geophys. Res. Lett.*, 7, 157-160, 1980.
- Langematz, U.: Stratospheric ozone: down and up through the Anthropocene, *ChemTexts* 5, 8, <https://doi.org/10.1007/s40828-019-0082-7>, 2019



- 840 Lanzante, J. R.: Resistant, robust and non-parametric techniques for the analysis of climate data: Theory and examples, including applications to historical radiosonde station data, *Int. J. Climatol.*, 16(11), 1197–1226, doi:10.1002/(SICI)1097-0088(199611)16:11<1197::AID-JOC89>3.0.CO;2-L, 1996.
- Lefohn, A. S., Malley, C. S., Smith, L., Wells, B., Hazucha, M., Simon, H., Naik, V., Mills, G., Schultz, M. G., Paoletti, E., De Marco, A., Xu, X., Zhang, L., Wang, T., Neufeld, H. S., Musselman, R. C., Tarasick, D., Brauer, M., Feng, Z., Tang, H.,
- 845 Kobayashi, K., Sicard, P., Solberg, S. and Gerosa, G.: Tropospheric ozone assessment report: Global ozone metrics for climate change, human health, and crop/ecosystem research, *Elem Sci Anth*, 6(1), p.28, doi: <http://doi.org/10.1525/elementa.279>, 2018.
- Lefever, K., van der A, R., Baier, F., Christophe, Y., Errera, Q., Eskes, H., Flemming, J., Inness, A., Jones, L., Lambert, J.-C., Langerock, B., Schultz, M. G., Stein, O., Wagner, A., and Chabrillat, S.: Copernicus stratospheric ozone service, 2009–
- 850 2012: validation, system intercomparison and roles of input data sets, *Atmos. Chem. Phys.*, 15, 2269–2293, <https://doi.org/10.5194/acp-15-2269-2015>, 2015.
- Lemoine, René and De Backer, H.: Assessment of the Uccle ozone sounding time series quality using SAGE II data, *J. Geophys. Res.*, 106, 14515–14523, 2001.
- Livesey, N. J., Read, W. G., Wagner, P. A., Froidevaux, L., Lambert, A., Manney, G. L., Millán Valle, L. F., Pumphrey, H.
- 855 C., Santee, M. L., Schwartz, M. J., Wang, S., Fuller, R. A., Jarnot, R. F., Knosp, B. W., Martinez, E., Lay, R. R. : EOS MLS Version 4.2x Level 2 and 3 data quality and description document, JPL D-33509 Rev. E. [Available at https://mls.jpl.nasa.gov/data/v4-2_data_quality_document.pdf], 2020.
- McPeters, R. D. and Labow, G. J.: Climatology 2011: An MLS and sonde derived ozone climatology for satellite retrieval algorithms, *J. Geophys. Res.-Atmos.*, 117, D10303, doi:10.1029/2011JD017006, 2012.
- 860 Monks, P. S., Archibald, A. T., Colette, A., Cooper, O., Coyle, M., Derwent, R., Fowler, D., Granier, C., Law, K. S., Mills, G. E., Stevenson, D. S., Tarasova, O., Thouret, V., von Schneidemesser, E., Sommariva, R., Wild, O., and Williams, M. L.: Tropospheric ozone and its precursors from the urban to the global scale from air quality to short-lived climate forcer, *Atmos. Chem. Phys.*, 15, 8889–8973, <https://doi.org/10.5194/acp-15-8889-2015>, 2015.
- Morgenstern, O., Hegglin, M. I., Rozanov, E., O'Connor, F. M., Abraham, N. L., Akiyoshi, H., Archibald, A. T., Bekki, S.,
- 865 Butchart, N., Chipperfield, M. P., Deushi, M., Dhomse, S. S., Garcia, R. R., Hardiman, S. C., Horowitz, L. W., Jöckel, P., Josse, B., Kinnison, D., Lin, M., Mancini, E., Manyin, M. E., Marchand, M., Marécal, V., Michou, M., Oman, L. D., Pitari, G., Plummer, D. A., Revell, L. E., Saint-Martin, D., Schofield, R., Stenke, A., Stone, K., Sudo, K., Tanaka, T. Y., Tilmes, S., Yamashita, Y., Yoshida, K., and Zeng, G.: Review of the global models used within phase 1 of the Chemistry–Climate Model Initiative (CCMI), *Geosci. Model Dev.*, 10, 639–671, <https://doi.org/10.5194/gmd-10-639-2017>, 2017.
- 870 Morris, G. A., Komhyr, W. D., Hirokawa, J., Flynn, J., Lefer, B., Krotkov, N., and Ngan, F.: A Balloon Sounding Technique for Measuring SO₂ Plumes. *J. Atmos. Oceanic Technol.*, 27, 1318–1330, <https://doi.org/10.1175/2010JTECHA1436.1>, 2010.



- Munro, R., Lang, R., Klaes, D., Poli, G., Retscher, C., Lindstrot, R., Huckle, R., Lacan, A., Grzegorski, M., Holdak, A., Kokhanovsky, A., Livschitz, J., and Eisinger, M.: The GOME-2 instrument on the Metop series of satellites: instrument
875 design, calibration, and level 1 data processing – an overview, *Atmos. Meas. Tech.*, 9, 1279–1301,
<https://doi.org/10.5194/amt-9-1279-2016>, 2016.
- Nassar, R., Logan, J. A., Worden, H. M., Megretskaia, I. A., Bowman, K. W., Osterman, G. B., Thompson, A. M., Tarasick,
D. W., Austin, S., Claude, H., Dubey, M. K., Hocking, W. K., Johnson, B. J., Joseph, E., Merrill, J., Morris, G. A.,
Newchurch, M., Oltmans, S. J., Posny, F., Schmidlin, F., Vömel, H., Whiteman, D. N., and Witte, J. C.: Validation of
880 tropospheric emission spectrometer (TES) nadir ozone profiles using ozonesonde measurements, *J. Geophys. Res.*, 113,
D15S17, doi:10.1029/2007JD008819, 2008.
- Osterman, G., Kulawik, S. S., Worden, H. M., Richards, N. A. D., Fisher, B. M., Eldering, A., Shephard, M. W., Froidevaux,
L., Labow, G., Luo, M., Herman, R. L., Bowman, K. W., and Thompson, A. M.: Validation of Tropospheric Emission
Spectrometer (TES) measurements of the total, stratospheric and tropospheric column abundance of ozone, *J. Geophys. Res.*,
885 113, D15S16, doi:10.1029/2007JD008801, 2008.
- Paoletti, E., De Marco, A., Beddows, D. C. S., Harrison, R. M., and Manning, W. J.: Ozone levels in European and USA
cities are increasing more than at rural sites, while peak values are decreasing, *Environ. Pollut.* 192: 295–299. doi:
<https://doi.org/10.1016/j.envpol.2014.04.040>, 2014.
- Parrish, D. D., Derwent, R. G., Steinbrecht, W., Stübi, R., Van Malderen, R., Steinbacher, M., Trickl, T., Ries, L., and Xu,
890 X.: Zonal Similarity of Long-term Changes and Seasonal Cycles of Baseline Ozone at Northern Mid-latitudes, *J. Geophys.*
Res.-Atmos., 125, e2019JD031908, <https://doi.org/10.1029/2019JD031908>, 2020.
- Petetin, H., Thouret, V., Fontaine, A., Sauvage, B., Athier, G., Blot, R., Boulanger, D., Cousin, J.-M., and Nédélec, P.:
Characterising tropospheric O₃ and CO around Frankfurt over the period 1994–2012 based on MOZAIC–IAGOS aircraft
measurements, *Atmos. Chem. Phys.*, 16, 15147–15163, <https://doi.org/10.5194/acp-16-15147-2016>, 2016.
- 905 Philipona, R., Mears, C., Fujiwara, M., Jeannot, P., Thorne, P., Bodeker, G., Haimberger, L., Hervo, M., Popp, C.,
Romanens, G., Steinbrecht, W., Stübi, R., and Van Malderen, R.: Radiosondes show that after decades of cooling, the lower
stratosphere is now warming, *J. Geophys. Res.-Atmos.*, 123, 12,509–12,522. <https://doi.org/10.1029/2018JD028901>, 2018.
- Rao, T. N., Arvelius, J., and Kirkwood, S.: Climatology of tropopause folds over a European Arctic station (Esrangle), *J.*
Geophys. Res., 113, D00B03, doi:10.1029/2007JD009638, 2008.
- 900 Rodgers, C. D.: Inverse methods for atmospheric sounding – theory and practice, Series on Atmospheric, Oceanic and
Planetary Physics, World Scientific Publishing, London, 2000.
- Santer, B. D., Wehner, M. F., Wigley, T. M. L., Sausen, R., Meehl, G. A., Taylor, K. E., Ammann, C., Arblaster, J.,
Washington, W. M., Boyle, J. S., and Brüggemann, W.: Contributions of Anthropogenic and Natural Forcing to Recent
Tropopause Height Changes, *Science*, 301, 479–483, <https://doi.org/10.1126/science.1084123>, 2003.
- 905 Sen, P. K.: Estimates of the regression coefficient based on Kendall’s tau, *J. Amer. Statist. Ass.*, 63: 1379–1389,
<https://doi.org/10.1080/01621459.1968.10480934>, 1968.



- Smit, H. G. J., Oltmans, S., Deshler, T., Tarasick, D., Johnson, B., Schmidlin, F., Stübi, R., and Davies, J.: SI2N/O3S-DQA Activity: Guide Lines for Homogenization of Ozone Sonde Data, version 19 November 2012, available at: http://www-das.uwyo.edu/~deshler/NDACC_O3Sondes/O3s_DQA/O3S-DQA-Guidelines%20Homogenization-V2-19November2012.pdf, 2012.
- 910 Smit, H.G.J., and ASOPOS panel: Quality assurance and quality control for ozonesonde measurements in GAW, WMO Global Atmosphere Watch report series, No. 121, 100 pp., World Meteorological Organization, GAW Report No. 201 (2014), 100 pp., Geneva. [Available online at https://library.wmo.int/pmb_ged/gaw_201_en.pdf], 2014.
- SPARC/IO3C/GAW: SPARC/IO3C/GAW Report on Long-term Ozone Trends and Uncertainties in the Stratosphere. I.
- 915 Petropavlovskikh, S. Godin-Beekmann, D. Hubert, R. Damadeo, B. Hassler, V. Sofieva (Eds.), SPARC Report No. 9, GAW Report No. 241, WCRP-17/2018, doi: 10.17874/f899e57a20b, available at www.sparc-climate.org/publications/sparc-reports, 2019.
- Stauffer, R. M., Morris, G. A., Thompson, A. M., Joseph, E., Coetzee, G. J. R., and Nalli, N. R.: Propagation of radiosonde pressure sensor errors to ozonesonde measurements, *Atmos. Meas. Tech.*, 7, 65–79, doi:10.5194/amt-7-65-2014, 2014.
- 920 Stauffer, R. M., Thompson, A. M., Kollonige, D. E., Witte, J. C., Tarasick, D. W., Davies, J., Vömel, H., Morris, G. A., Van Malderen, R., Johnson, B. J., Querel, R. R., Selkirk, H. B., Stübi, R., and Smit, H. G. J.: A Post-2013 Drop-off in Total Ozone at a Third of Global Ozonesonde Stations: ECC Instrument Artifacts?, *Geophys. Res. Lett.*, 47, e2019GL086791, <https://doi.org/10.1029/2019GL086791>, 2020.
- Steinbrecht, W., Claude, H., Schönborn, F., Leiterer, U., Dier, H. and Lanzinger, E.: Pressure and temperature differences between Vaisala RS80 and RS92 radiosonde systems, *J. Atmos. Ocean. Tech.*, 25, 909–927, 2008.
- 925 Sterling, C. W., Johnson, B. J., Oltmans, S. J., Smit, H. G. J., Jordan, A. F., Cullis, P. D., Hall, E. G., Thompson, A. M., and Witte, J. C.: Homogenizing and estimating the uncertainty in NOAA's long-term vertical ozone profile records measured with the electrochemical concentration cell ozonesonde, *Atmos. Meas. Tech.*, 11, 3661–3687, <https://doi.org/10.5194/amt-11-3661-2018>, 2018.
- 930 Stübi, R., Levrat, G., Hoegger, B., Viatte, P., Staehelin, J., and Schmidlin, F. J.: In-flight comparison of Brewer-Mast and electrochemical concentration cell ozonesondes, *J. Geophys. Res.*, 113, D13302, doi:10.1029/2007JD009091, 2008.
- Tarasick, D. W., Davies, J., Anlauf, K., Watt, M., Steinbrecht, W., and Claude, H. J.: Laboratory investigations of the response of Brewer-Mast ozonesondes to tropospheric ozone, *J. Geophys. Res.*, 107(D16), doi:10.1029/2001JD001167, 2002.
- 935 Tarasick, D. W., Davies, J., Smit, H. G. J., and Oltmans, S. J.: A re-evaluated Canadian ozonesonde record: measurements of the vertical distribution of ozone over Canada from 1966 to 2013, *Atmos. Meas. Tech.*, 9, 195–214, <https://doi.org/10.5194/amt-9-195-2016>, 2016.
- Tarasick, D. W., Carey-Smith, T. K., Hocking, W. K., Moeini, O., He, H., Liu, J., Osman, M. K., Thompson, A. M., Johnson, B. J., Oltmans, S. J., and Merrill, J. T.: Quantifying stratosphere-troposphere transport of ozone using balloon-



- 940 borne ozonesondes, radar windprofilers and trajectory models, *Atmos. Environ.*, 198, 496-509, <https://doi.org/10.1016/j.atmosenv.2018.10.040>, 2019.
- Tarasick, D. W., Smit, H. G. J., Thompson, A. M., Morris, G. A., Witte, J. C. Davies, J., Nakano, T., Van Malderen, R., Stauffer, R. M. Johnson, B. J., Stübi, R., Oltmans, S. J., and Vömel, H.: Improving ECC Ozonesonde Data Quality: Assessment of Current Methods and Outstanding Issues. *Earth and Space Science*, in revision, 2020.
- 945 Theil, H.: A rank-invariant method of linear and polynomial regression analysis, I. *Proc. Kon. Ned. Akad. v. Wetensch. A.* 53: 386–392, 1950a
- Theil, H.: A rank-invariant method of linear and polynomial regression analysis, II. *Proc. Kon. Ned. Akad. v. Wetensch. A.* 53: 521–525, 1950b
- Theil, H.: A rank-invariant method of linear and polynomial regression analysis, III. *Proc. Kon. Ned. Akad. v. Wetensch. A.*
- 950 53: 1397–1412, 1950c
- Thompson, A. M., Oltmans, S. J., Tarasick, D. W., von der Gathen, P., Smit, H. G. J., and Witte, J. C.: Strategic ozone sounding networks: Review of design and accomplishments, *Atmos. Environ.*, 45, 2145–2163, <https://doi.org/10.1016/j.atmosenv.2010.05.002>, 2011
- Thompson, A. M., Witte, J. C., Sterling, C., Jordan, A., Johnson, B. J., Oltmans, S. J., Fujiwara, M., Vömel, H., Allaart, M.,
- 955 Pitters, A., Coetzee, G. J. R., Posny, F., Corrales, E., Diaz, J. A., Félix, C., Komala, N., Lai, N., Hoang Ahn, N. T., Maata, M., Mani, F., Zainal, Z., Ogino, S., Paredes, F., Penha, T. L. B. da Silva, F. R., Sallons-Mitro, S., Selkirk, H. B., Schmidlin, F. J., Stübi, R., and Thiong'o, K.: First reprocessing of Southern Hemisphere Additional Ozonesondes (SHADOZ) ozone profiles (1998–2016): 2. Comparisons with satellites and ground-based instruments, *J. Geophys. Res.-Atmos.*, 122, 13,000–13,025. <https://doi.org/10.1002/2017JD027406>, 2017.
- 960 Thompson, A. M., Smit, H. G., Witte, J. C., Stauffer, R. M., Johnson, B. J., Morris, G., von der Gathen, P., Van Malderen, R., Davies, J., Pitters, A., Allaart, M., Posny, F., Kivi, R., Cullis, P., Hoang Anh, N. T., Corrales, E., Machinini, T., da Silva, F. R., Paiman, G., Thiong'o, K., Zainal, Z., Brothers, G. B., Wolff, K. R., Nakano, T., Stübi, R., Romanens, G., Coetzee, G. J., Diaz, J. A., Sallons-Mitro, S., Mohamad, M., and Ogino, S.: Ozonesonde Quality Assurance: The JOSIE–SHADOZ (2017) Experience, *B. Am. Meteorol. Soc.*, 100, 155–171, <https://doi.org/10.1175/BAMS-D-17-0311.1>, 2019.
- 965 Tie, X., and Brasseur, G.: The response of stratospheric ozone to volcanic eruptions: Sensitivity to atmospheric chlorine loading. *Geophys. Res. Lett.*, 22, 3035–3038, <https://doi.org/10.1029/95GL03057>, 1995.
- Tørseth, K., Aas, W., Breivik, K., Fjæraa, A. M., Fiebig, M., Hjellbrekke, A. G., Lund Myhre, C., Solberg, S., and Yttri, K. E.: Introduction to the European Monitoring and Evaluation Programme (EMEP) and observed atmospheric composition change during 1972–2009, *Atmos. Chem. Phys.*, 12, 5447–5481, <https://doi.org/10.5194/acp-12-5447-2012>, 2012.
- 970 Valks, P., Hao, N., Gimeno Garcia, S., Loyola, D., Dameris, M., Jöckel, P., and Delcloo, A.: Tropical tropospheric ozone column retrieval for GOME-2, *Atmos. Meas. Tech.*, 7, 2513–2530, <https://doi.org/10.5194/amt-7-2513-2014>, 2014.
- Van Haver Ph., De Muer, D., Beekmann, M. and Mancier, C.: Climatology of tropopause folds at midlatitudes, *Geophys. Res. Lett.*, 23, pp. 1033-1036, doi: 10.1029/96GL00956, 1996.



- Van Malderen, R., and De Backer, H.: A drop in upper tropospheric humidity in autumn 2001, as derived from
975 radiosonde measurements at Uccle, Belgium, *J. Geophys. Res.-Atmos.*, 115, D20114, doi:10.1029/2009JD013587, 2010.
- Van Malderen, R., Allaart, M. A. F., De Backer, H., Smit, H. G. J., and De Muer, D.: On instrumental errors and related
correction strategies of ozonesondes: possible effect on calculated ozone trends for the nearby sites Uccle and De Bilt,
Atmos. Meas. Tech., 9, 3793–3816, doi:10.5194/amt-9-3793-2016, 2016.
- van Peet, J. C. A., van der A, R. J., Tuinder, O. N. E., Wolfram, E., Salvador, J., Levelt, P. F., and Kelder, H. M.: Ozone
980 Profile Retrieval Algorithm (OPERA) for nadir-looking satellite instruments in the UV–VIS, *Atmos. Meas. Tech.*, 7, 859–
876, <https://doi.org/10.5194/amt-7-859-2014>, 2014.
- Verstraeten, W.W., Boersma, K. F., Zörner, J., Allaart, M. A. F., Bowman, K. W., and Worden, J. R.: Validation of six years
of TES tropospheric ozone retrievals with ozonesonde measurements: implications for spatial patterns and temporal stability
in the bias, *Atmos. Meas. Tech.*, 6, 1413–1423, <https://doi.org/10.5194/amt-6-1413-2013>, 2013.
- 985 Verstraeten, W. W., Neu, J. L., Williams, J. E., Bowman, K. W., Worden, J. R., and Boersma, K. F.: Rapid increases in
tropospheric ozone production and export from China, *Nat. Geosci.*, 8, 690–695, <https://doi.org/10.1038/ngeo2493>, 2015.
- Wargan, K., Orbe, C., Pawson, S., Ziemke, J. R., Oman, L. D., Olsen, M. A., Coy, L., and Emma Knowland, K.: Recent
Decline in Extratropical Lower Stratospheric Ozone Attributed to Circulation Changes, *Geophys. Res. Lett.*, 45, 5166–5176,
<https://doi.org/10.1029/2018GL077406>, 2018.
- 990 Weber, M., Coldewey-Egbers, M., Fioletov, V. E., Frith, S. M., Wild, J. D., Burrows, J. P., Long, C. S., and Loyola, D.:
Total ozone trends from 1979 to 2016 derived from five merged observational datasets – the emergence into ozone recovery,
Atmos. Chem. Phys., 18, 2097–2117, <https://doi.org/10.5194/acp-18-2097-2018>, 2018.
- Witte, J. C., Thompson, A. M., Smit, H. G. J., Fujiwara, M., Posny, F., Coetzee, G. J. R., Northam, E. T., Johnson, B. J.,
Sterling, C. W., and Mohamad, M.: First reprocessing of Southern Hemisphere Additional OZonesondes (SHADOZ) profile
995 records (1998–2015): 1. Methodology and evaluation, *J. Geophys. Res.-Atmos.*, 122, 6611–6636,
<https://doi.org/10.1002/2016JD026403>, 2017.
- Witte, J. C., Thompson, A. M., Smit, H. G. J., Vömel, H., Posny, F., and Stübi, R.: First reprocessing of Southern
Hemisphere ADditional OZonesondes profile records: 3. Uncertainty in ozone profile and total column, *J. Geophys. Res.-
Atmos.*, 123, 3243–3268, <https://doi.org/10.1002/2017JD027791>, 2018.
- 1000 Witte, J. C., Thompson, A. M., Schmidlin, F. J., Northam, E. T., Wolff, K. R., and Brothers, G. B.: The NASA Wallops
Flight Facility digital ozonesonde record: Reprocessing, uncertainties, and dual launches, *J. Geophys. Res.-Atmos.*, 124,
3565–3582, <https://doi.org/10.1029/2018JD030098>, 2019.
- World Meteorological Organization (WMO), *Meteorology—A three dimensional science: Second session of the
Commission for Aerology*, World Meteorol. Organ. Bull., IV(4), 134–138, 1957.
- 1005 World Meteorological Organization (WMO), *Third WMO intercomparison of the ozonesondes used in the Global Ozone
Observing System* (Vanscoy, Canada 13–24 May 1991, Global Ozone Research and Monitoring Project, Rep. 27, Geneva,
1991.



- WMO (World Meteorological Organization), Scientific Assessment of Ozone Depletion: 2014, Global Ozone Research and Monitoring Project – Report No. 55, 416 pp., Geneva, Switzerland, 2014.
- 1010 WMO (World Meteorological Organization), Scientific Assessment of Ozone Depletion: 2018, Global Ozone Research and Monitoring Project – Report No. 58, 588 pp., Geneva, Switzerland, 2018.
- Xian, T. and Homeyer, C. R.: Global tropopause altitudes in radiosondes and reanalyses, *Atmos. Chem. Phys.*, 19, 5661–5678, <https://doi.org/10.5194/acp-19-5661-2019>, 2019.
- Yan, Y., Pozzer, A., Ojha, N., Lin, J., and Lelieveld, J.: Analysis of European ozone trends in the period 1995–2014, *Atmos. Chem. Phys.*, 18, 5589–5605, <https://doi.org/10.5194/acp-18-5589-2018>, 2018.
- 1015 Young, P. J., Naik, V., Fiore, A. M., Gaudel, A., Guo, J., Lin, M. Y., Neu, J. L., Parrish, D. D., Rieder, H. E., Schnell, J. L., Tilmes, S., Wild, O., Zhang, L., Ziemke, J. R., Brandt, J., Delcloo, A., Doherty, R. M., Geels, C., Hegglin, M. I., Hu, L., Im, U., Kumar, R., Luhar, A., Murray, L., Plummer, D., Rodriguez, J., Saiz-Lopez, A., Schultz, M. G., Woodhouse, M. T. and Zeng, G.: Tropospheric Ozone Assessment Report: Assessment of global-scale model performance for global and regional
- 1020 ozone distributions, variability, and trends, *Elem Sci Anth*, 6(1), p.10. doi: <http://doi.org/10.1525/elementa.265>, 2018.